PALAIOS
Emphasizing the impact of life on Earth's history

PALAIOS, 2023, v. 38, 1–21
Research Article
DOI: http://dx.doi.org/10.2110/palo.2022.025

THE TAPHONOMIC CHARACTER, OCCURRENCE, AND PERSISTENCE OF UPPER PERMIAN–LOWER TRIASSIC PLANT ASSEMBLAGES IN THE MID-PALEOLATITUDES, BOGDA MOUNTAINS, WESTERN CHINA

ROBERT A. GASTALDO,[1] MINGLI WAN,[2] AND WAN YANG[3]
[1]*Department of Geology, Colby College, Waterville, Maine, 04901 USA*
[2]*State Key Laboratory of Palaeobiology and Stratigraphy, Center for Excellence in Life and Paleoenvironment, Nanjing Institute of Geology and Palaeontology, Chinese Academy of Sciences, Nanjing, 210008, China*
[3]*Geology and Geophysics Program, Missouri University of Science and Technology, Rolla, Missouri 65409, USA*
email: ragastal@colby.edu

ABSTRACT: **The Bogda Mountains, Xianjiang Uygur Autonomous Region, western China, expose an uppermost Permian–Lower Triassic succession of fully continental strata deposited across three graben (half graben) structures in the mid-paleolatitudes of Pangea. A cyclostratigraphy scheme developed for the succession is subdivided into three low-order cycles (Wutonggou, Jiucaiyuan, Shaofanggou). Low-order cycles are partitioned into 1838 high-order cycles based on repetitive environmental changes, and their plant taphonomic character is assessed in $>$ 4700 m of high-resolution, measured sections distributed across $\sim$ 100 km. Four taphonomic assemblages are represented by: permineralized wood (both autochthonous and allochthonous), megafloral adpressions (?parautochthonous and allochthonous) identifiable to systematic affinity, unidentifiable (allochthonous) phytoclasts concentrated or disseminated on bedding, and (autochthonous) rooting structures of various configurations (carbon films to rhizoconcretions). Their temporal and spatial occurrences vary across the study area and are dependent on the array of depositional environments exposed in any particular locality.**

Similar to paleobotanical results in other fully continental basins, megafloral elements are rarely encountered. Both wood (erect permineralized stumps and prostrate logs) and adpressions are found in $<$ 2% of meandering river and limnic cycles, where sediment accumulated under semi-arid to humid conditions. The absence of such assemblages in river-and-lake deposits is more likely related to physical or geographical factors than it is to an absence of organic-matter contribution. With such a low frequency, no predictable pattern or trend to their occurrence can be determined. This is also true for any horizon in which rooting structures are preserved, although paleosols occur in all or parts of high-order cycles developed under arid to humid conditions. Physical rooting structures are encountered in only 23% of these and are not preserved equally across space and time. Allochthonous phytoclasts are the most common taphonomic assemblage, preserved in association with micaceous minerals on bedding in fine-grained lithofacies. The consistency of phytoclast assemblages throughout the succession is empirical evidence for the presence of riparian vegetation during a time when models propose the catastrophic demise of land plants, and does not support an interpretation of vegetational demise followed by long-term recovery across the crisis interval in this basin. These mesofossil and microfossil (palynological) assemblages offer the best opportunity to understand the effects of the crisis on the base of terrestrial ecosystems.

INTRODUCTION

Higher plants form the base of terrestrial ecosystems with changes in diversity, community composition and structure, and geographic distribution directly impacting both invertebrate and vertebrate groups over various temporal scales. The plant-fossil record is critical to, and forms the basis of, our interpretations of the dynamics associated with Phanerozoic continental extinctions since plant communities colonized and expanded their phytogeographic distribution in their conquest of land. Yet, the paleontological windows into megafloral trends and their interpreted responses over time are dependent on many inter-related factors. These include, but are not limited to: the taphonomic conditions and depositional context of each assemblage used in the analysis; regional tectonic, climatic, and sedimentologic dynamics controlling the stratigraphic record in any particular basin at various paleolatitudes; and the availability, extent, and quality of exposure from which fossil assemblages can be collected and assessed. Each factor, individually and collectively, impart one or more biases that must be taken into consideration during data synthesis and interpretation (e.g., Behrensmeyer et al. 2000; DiMichele and Gastaldo 2008). Our understanding of the response of plant communities and biomes to the end-Permian terrestrial crisis is no exception.

The response of terrestrial ecosystems during the end-Permian crisis has been interpreted by several workers as a universally catastrophic, domino-style event across continents and paleohemispheres. The decimation, extirpation, and extinction of land plants over a short temporal duration is interpreted as having cascaded through global community structures resulting in critical losses of, particularly, vertebrate assemblages (e.g., Smith and Botha-Brink 2014; Roopnarine et al. 2019; Viglietti et al. 2021). End-Permian continental events are reported to have been temporally coincident (e.g., Benton and Newell 2014) with phased marine-extinction

Published Online: January 2023
 0883-1351/23/038-1

pulses (e.g., Shen et al. 2019) over a tightly constrained geochronometric interval of 60–120 ky interval (Burgess et al. 2014). More recently, regional-scale variance in latest Permian to Early Triassic floral trends has been documented over this critical time interval in both the northern (e.g., Chu et al. 2016; Davydov et al. 2021; Yang et al. 2021; Tabor et al. 2022) and southern paleohemispheres (e.g., Schneebeli-Hermann 2020; Gastaldo et al. 2021; Fielding et al. 2022). A similar pattern is reflected in data compiled on a global basis (Nowak et al. 2019; Lucas 2021). One basin where the paleobotanical record is preserved in a fully continental basin that spans the Permian–Triassic Boundary (PTB) is in western China.

The foothills of the Bogda Mountains, Xinjiang Uyghur Autonomous Region, China (Fig. 1A), host an early Permian to Middle Triassic record of rift-basin deposits exposed in a large anticline, separating the Turpan-Hami Basin to the south from the Junggar Basin to the north–northwest. The cyclostratigraphy of the Bogda records consists of three orders (high, intermediate, and low) of sedimentary cycles. High-order cycles (HCs) are defined on the basis of repetitive changes of fluvial and lacustrine environments and are regarded as the smallest stratigraphic entity. Intermediate-order cycles (ICs) are composed of stacked high-order cycles deposited in a pattern of large-scale lake expansion and contraction or fluvial aggradation. Low-order cycles (LCs) contain similar ICs and reflect long-term trends of environmental, climatic, and/or tectonic conditions. LCs are bounded by regional unconformable, disconformable, and conformable surfaces and, thus, are interpreted as synchronous in the basin (Fig. 1B; Yang et al. 2007, 2010, 2021). Recent high-resolution U-Pb ID-TIMS ages constrain an age model across the PTB for these rocks in the Tarlong-Taodonggou region (Yang et al. 2021; Fig. 2), and provide a geochronological context. Here, we focus on the taphonomy and stratigraphic occurrence of upper Permian and Lower Triassic plant assemblages spread across localities that include Tarlong-Taodonggou (N43.2319°, E088.9733°) and Zhaobishan (N43.2495°, E090.4264°; Fig. 3) in the south and Dalongkou (N43.9617°, E 088.8705°; Fig. 4) in the north. Tarlong-Taodonggou is located ~ 80 km south of Dalongkou and ~ 100 km west of Zhaobishan. Our study seeks to determine: (1) how common the different types of plant-fossil assemblages are distributed and represented in correlative sections; (2) the relationships between taphonomic assemblages, depositional environments, and the prevailing climate at the time of preservation; and (3) how patterns of extinction and recovery are reflected in the Bogda Mountains in light of plant-fossil taphonomy.

GEOLOGICAL BACKGROUND

Uppermost Carboniferous–Triassic fluvial, floodplain, and lacustrine deposits are exposed along the northern, western, and southern foothills of the Bogda Mountains where they were deposited in intracontinental grabens of the Turpan-Junggar microplate (e.g., Yang et al. 2021). The microplate is located on the easternmost Kazakhstan Plate, which migrated northward to ~ 30–50°N paleolatitude during the early Permian to Early Triassic (Sengör and Natalín 1996). Grabens and half-grabens developed on Carboniferous volcanic-arc and oceanic basement in a tectonic setting similar to the Neogene Basin-and-Range Province, western U.S. (e.g., Yang 2008; Yang et al. 2010, 2013). These basins were filled by clastic sediments with their provenance from local horsts and the northern Tianshan suture zone (Shao et al. 2001; Zheng and Yang 2020). The conformable succession of middle Permian to Lower Triassic fluvial-lacustrine deposits and paleosols is bounded by a lower (Wordian) and an upper (Olenekian) major unconformity (Fig. 1B). These rocks overlie lower Permian alluvial, fluvial, and lacustrine sediments that formed under stages of early rifting, and underlie Middle Triassic braided stream deposits (Yang et al. 2010; Obrist-Farner and Yang 2017).

Yang et al. (2007, 2010, 2021) recognize six major transition zones, based on environmental, tectonic, climatic, and paleontologic criteria, that are organized into five intervals constituting the middle Permian–Lower Triassic record. This record accumulated in at least three separate grabens, or half grabens, and represent approximately 5 Ma of sedimentation. Each interval is defined as a low-order sedimentary cycle (LC; Fig. 1B), and represents a period of regional, long-term tectonic, climatic, and environmental stability. The lower (Wordian) unconformity marks a major regional uplift whereby lacustrine deposits of the Hongyanchi LC are terminated and followed by fluvial peneplanation and deposition of the lower Quanzijie LC (Obrist-Farner and Yang 2015). This is followed by loess-fluvial deposition of the upper Quanzijie LC and fluvial-lacustrine deposition of, in ascending order, the Wutonggou, Jiucaiyuan, and Shaofanggou LCs in enlarged grabens. The upper bounding unconformity (Olenekian) reflects regional uplift over which thick, anabranching fluvial systems deposited sediments of the lower part of the Middle Triassic Karamay LC. Major unconformities were the result of changing tectonic regimes. In contrast, conformable environmental transitions in LCs relate mainly to changes in climatic, sedimentary systems and their associated landscapes, and catchment conditions (Yang et al. 2021). Thus, trends in depositional environments and climate were linked closely during the deposition of the middle Permian to Lower Triassic succession.

LOCALITIES, STRATIGRAPHY, DEPOSITIONAL ENVIRONMENTS

Taodonggou/Tarlong

Yang et al. (2007, 2010, 2021) described seven middle Permian to Lower Triassic sections situated on the flanks of large anticlines in the region northwest of Turpan (Fig. 2A). The most complete successions occur in northern and southern Tarlong (~ 1000 and 900 m thick, respectively) and Taodonggou (~ 900 m) in the Tarlong-Taodonggou half graben (Fig. 2A). As a consequence of strong tectonism, the attitude of lithologies varies from low-to-moderate dips (~ 30–40°) near the hinge line of the syncline in South Tarlong (Fig. 2D) to high angle to near vertical dips (77°) in North Tarlong (Fig. 2C). In contrast, beds dip at relatively low angles (33°) in Taodonggou (Fig. 2B). Regional variation in sediment supply and accommodation resulted in differences in the thickness of measured sections across the region.

The thickest measured sections are found in the North Tarlong area where 826 m are reported and South Tarlong where 872 m are documented (Yang et al. 2021, supplemental data). The stratigraphic interval recorded in North Tarlong encompasses the Upper Quantzjie LC to the Wutonggou LC, whereas the interval including the Upper Quantzjie LC to the Jiucaiyuan LC is exposed in South Tarlong (Fig. 1). The stratigraphic thickness of the North and Central Taodonggou sections, including the Upper Quanzijie LC and lower and middle part of the Wutonggou LC, is 565.5 m. In contrast, 872 m and 295 m are documented in the South Tarlong and Southwest Tarlong sections, respectively. Here, the section includes the upper part of the Wutonggou LC to the lower part of the Shaofanggou LC (Fig. 1).

The uppermost Permian to Lower Triassic interval consists of a wide range of lithologies used to interpret various fully continental depositional environments. Lithologies range from clast-and-matrix supported coarse pebble/cobble conglomerate, coarse- to fine-grained sandstone (lithic wacke, subarenite and arenite), siltstone, mudstone, claystone, poor quality coal and carbonaceous shale. Rarely is lacustrine limestone encountered. Conglomerate and sandstone are the most resistant lithologies, standing in relief along outcrops (Fig. 2C, 2D). In contrast, fine-grained clastic intervals are highly fragmented and deeply weathered, with the depth of surficial weathering locally up to 1 m. Based on facies associations and accessory criteria, Yang et al. (2007, 2010, 2021) recognized a spectrum of fluvial (anabranching to coarse-grained meandering and [Gilbert-type] deltaic) and lacustrine systems (under-

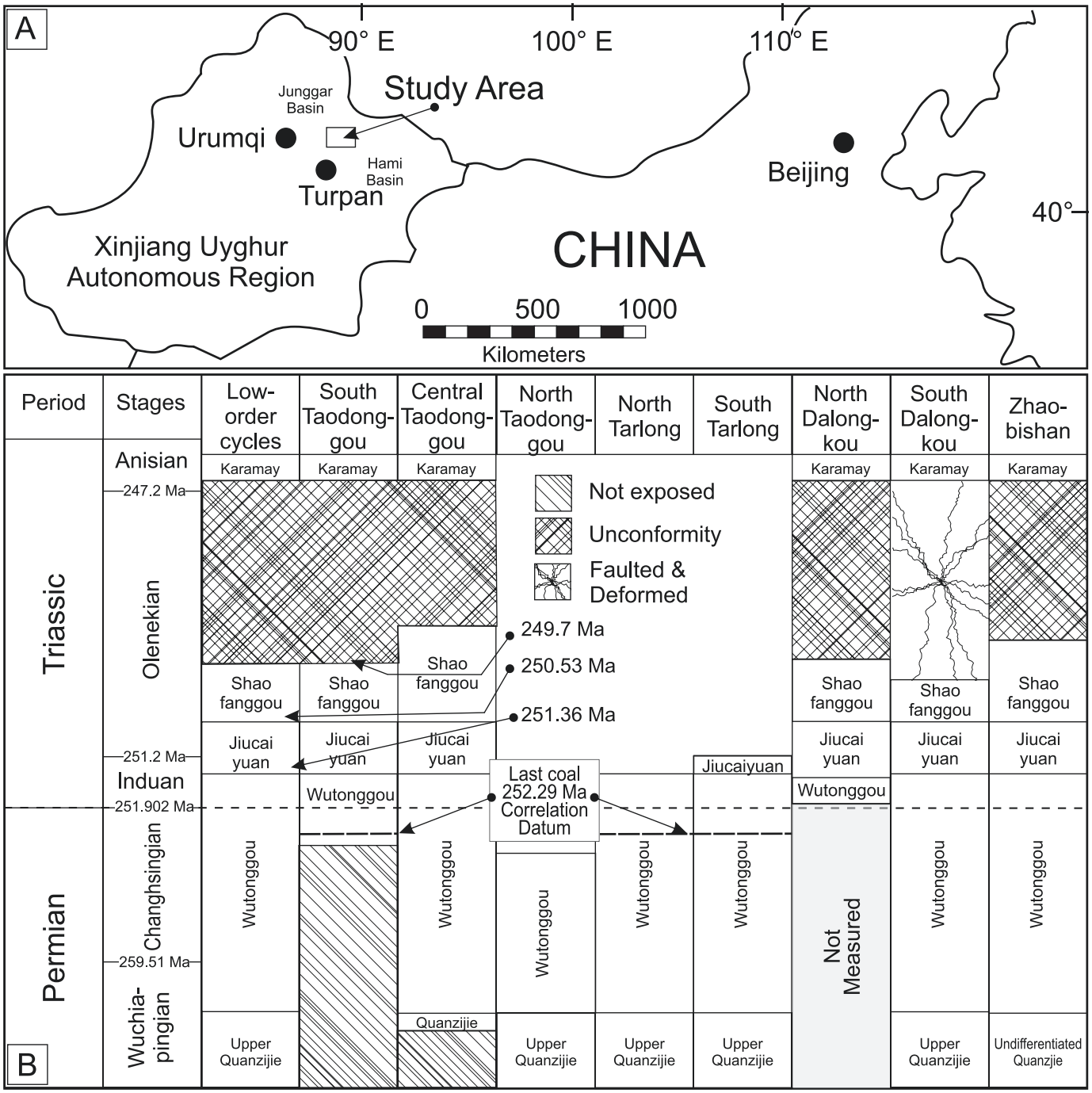

FIG. 1.—Study area, localities, and general stratigraphy. **A**) Map of NW China, NE Xinjiang Uyghur Autonomous Region, in which the study area is outlined. **B**) Upper Permian–Lower Triassic chrono-, litho-, and cyclo-stratigraphy of measured sections in the Tarlong-Taodonggou, Dalongkou, and Zhaobishan areas of the Bogda Mountains. Low-order cycles (LCs) and age estimates of LC boundaries are adapted from Yang et al. (2021) for North and South Tarlong and south Taodonggou sections, and projected into other localities using average sedimentation rates. The last occurrence of coal in the Wutonggou LC in Tarlong-Taodonggou and south Taodonggou is used as a correlation datum. Hatched intervals indicate major unconformities between the Shaofanggou and Karamay LCs.

filled to overfilled, delta-front and beach littoral sandstones; Bohacs et al. 2000). Based on soil morphology, structure, texture, and color, at least seven paleosols types were reported to occur (Thomas et al. 2011). When evaluated in stratigraphic succession, the stacking patterns of these facies are interpreted to represent cycles of fluvial-lacustrine, expansion-contraction, and environmental shifts related to variable allogenic-forcing mechanisms (tectonic, climatic).

Zhaobishan

Five measured sections are described on the flanks of a large syncline (Fig. 3A) situated to the northeast of ShanShan County (Yang et al. 2010, 2021). The thickest section measures 1140.5 m wherein the attitude of rocks reflects a moderate dip (50°) towards the syncline axis. Stratigraphically, these rocks encompass the interval from the Quanzjie to

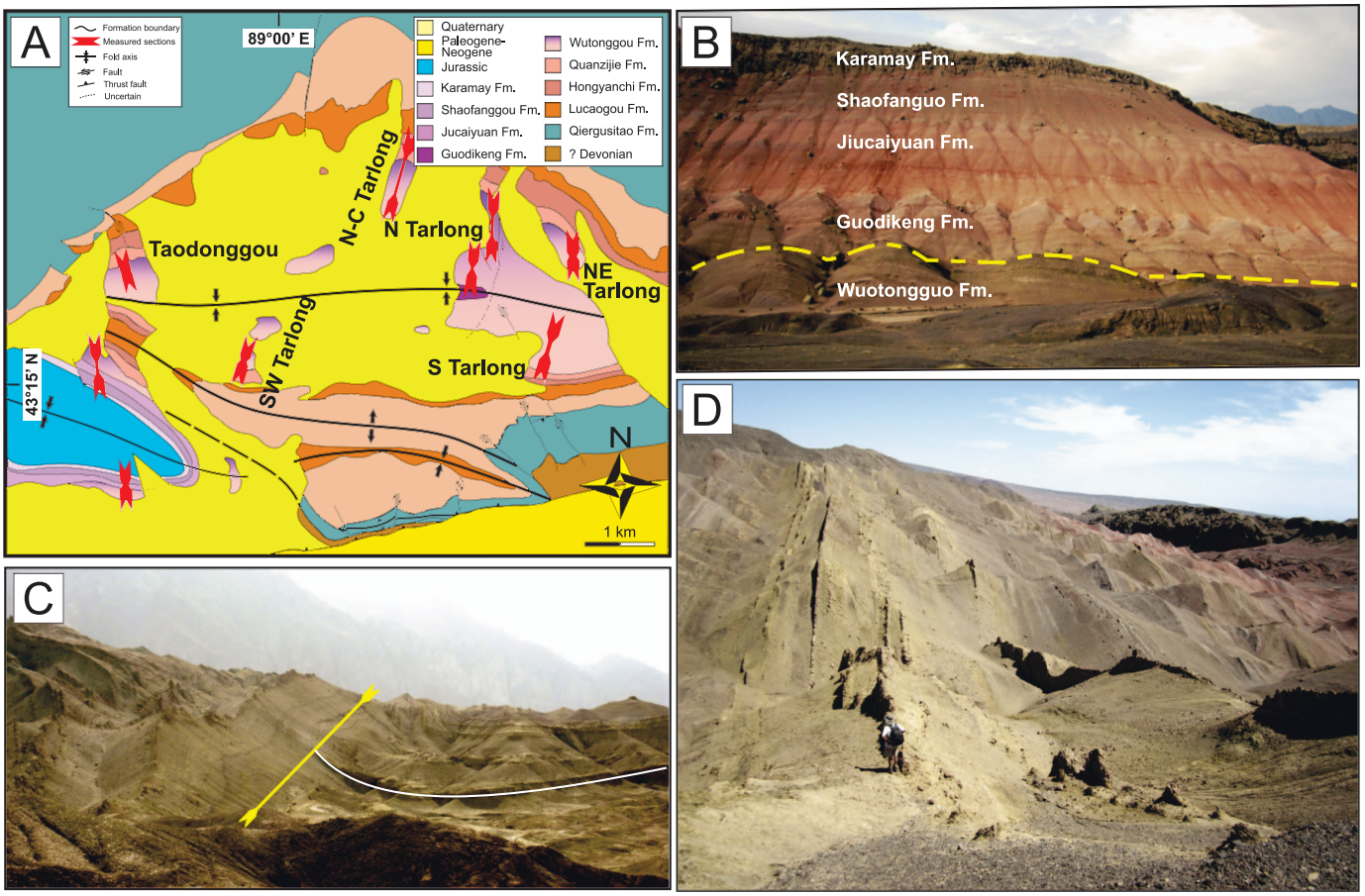

FIG. 2.—Tarlong-Taodonggou study area (N43.2319°, E088.9733°). **A**) Geologic map of NE Xinjiang showing study area and the approximate location of measured sections (red-arrow lines). Modified from Yang et al. (2021). **B**) Image looking north in Taodonggou where the uppermost Permian–Middle Triassic succession is exposed, and the approximate position of the Permian–Triassic Boundary (dashed yellow line), based on the age model of Yang et al. (2021). **C**) Image looking north in South Tarlong showing the deformed Wutonggou LC folded in the axis of a regional syncline terminated by a thrust fault (yellow line); a coal outcrops in the axis of the syncline. **D**) Deformed, high-angle beds exposed in Central Taodonggou.

Shaofanggou LC (Fig. 1). Lithologies in this half-graben structure are the same as those exposed in the Taodonggou /Tarlong area, and represent the same array of depositional environments. In contrast to these areas, the Zhaobishan section contains the greatest volume of conglomerate and sandstone. Resistant braided and coarse-grained meandering stream deposits are common and overlain by thick, retrogradational successions of individual coarsening-upward littoral-beach and lacustrine deltaic cycles (Fig. 3B). This is particularly true in the Jiucaiyuan LC, which is significantly different from those in both the Taodonggou and Dalongkou sections. Here, braided stream deposits comprise nearly half (50%) of the stratigraphic section, with subdominant (35%) lake-plain littoral deposits. Combined, these alternating fluvial-lacustrine successions define a second-order cyclicity (Yang et al. 2021). One localized feature of the Jiucaiyuan LC is the presence of a Calcisol in which a 30-cm thick, resistant, petrocalcic layer forms a giant gilgai/pseudo-anticline which has a ~ 20 m span and ~ 1 m relief (Yang et al. 2021). But, similar to localities described above, less competent, fine-grained clastic intervals are tectonically fractured and deeply weathered.

Dalongkou

The succession at Dalongkou has been studied by various workers (e.g., Afonin and Foster 2005; Foster and Afonin 2006) and has served as a touchstone for the PTB in western China (Metcalf et al. 2009). The outcrops are located to the southwest of Jimsar. The North (305 m) and South (413 m) measured sections of Yang et al. (2021) occur on the flanks of a large anticline (Fig. 4) where beds dip at low angles (24°) to nearly vertical attitudes. Similar to the other areas, the lithologies in this section range from coarse conglomerate to mudstone and represent the same array of depositional environments. These range from anabranching and high-relief rivers to lacustrine lake plain littoral and deltaic deposits to paleosols. Of note is the presence of calcic Argillisols in south Dalongkou (Yang et al. 2021). Similar to the stratigraphic interval exposed in Zhaobishan and elsewhere, tectonically fragmented and highly weathered rocks in Dalongkou occur throughout the Quanzijie to Upper Shaofanggou LCs (Fig. 1).

METHODS AND LOGISTICAL CONSTRAINTS

Beds in which plant fossils of various character and preservational states were noted by Yang et al. (2010, 2021) in their measured sections that serve as the basis for field work undertaken in the 2019 excursion. High-resolution, centimeter-scale lithologic descriptions, stacking pattern(s), and interpreted depositional environments are available in the supplemental documents accompanying these publications. Intervals in which "large" plant megafossils are reported in these sections were targeted and evaluated first in the field, and include beds where adpressions and permineralizations are preserved.

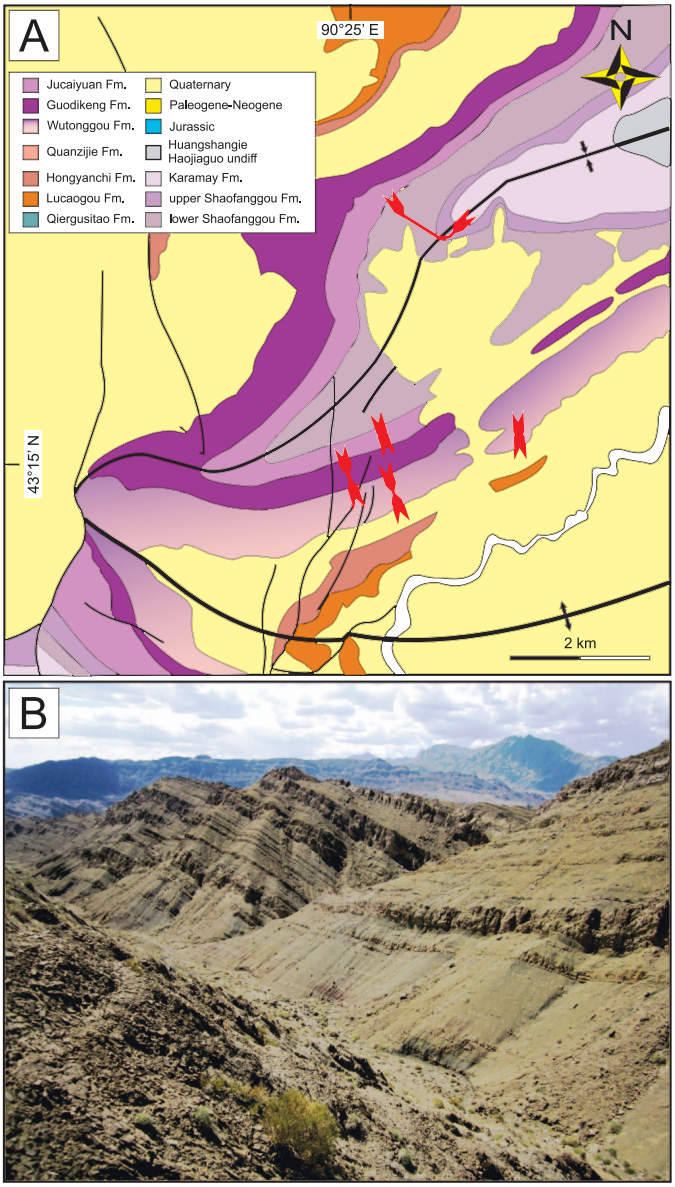

FIG. 3.—Zhaobishan study area (N43.2495°, E090.4264°). **A**) Geologic map of study area and the approximate location of measured sections (red-arrow lines). Modified from Yang et al. (2021). **B**) Thick succession of rift-lake deposits assigned to the Wutonggou and Juicaiyuan LCs, where sandstones remain more resistant to weathering than the intervening shale, siltstone, and mudstone.

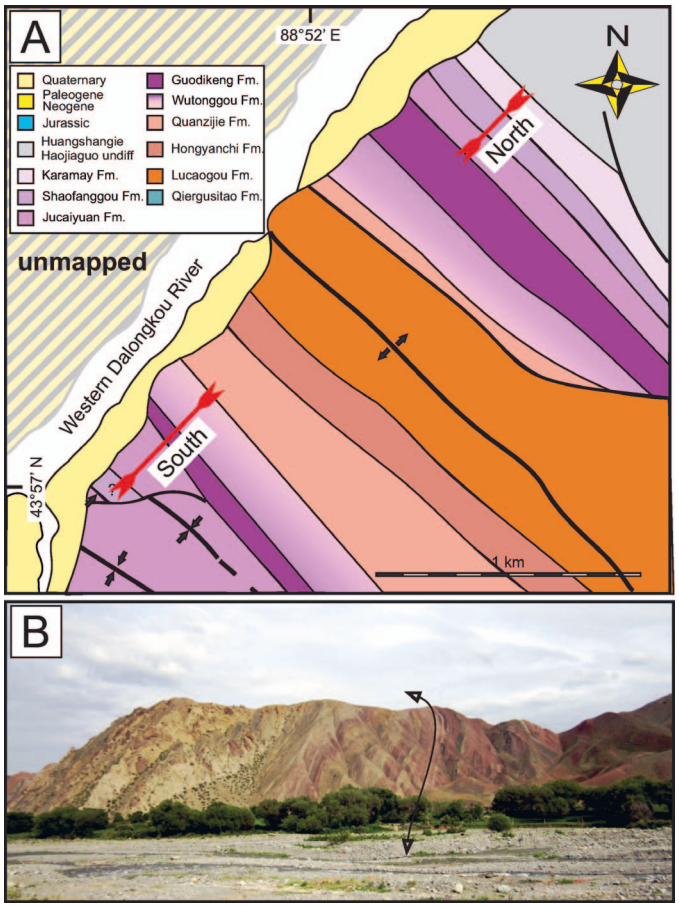

FIG. 4.—Dalongkou study area (N43.9617°, E088.8705°). **A**) Geologic map showing study area and the approximate location of measured South and North Dalongkou sections (red-arrow lines). Modified from Obrist-Farner and Yang (2015) and Yang et al. (2021). **B**) Image of the deformed, classic (Metcalf et al. 2009) South Dalongkou succession exposed in an anticline (double-headed arrow) adjacent to the West Dalongkou River near Jimsar, China.

The highly deformed nature, and moderate-to-high dip of beds in the Bogda Mountains complicates the recovery of adpression assemblages where preserved. The confining pressures of competent rock above and below any fossil-bearing bed or short stratigraphic interval prevent recovery of little more than fragments that, commonly, are no more than a few centimeters in any dimension. Where less competent rock is found, rock fragments recovered from the subsurface are on the order of less than 5–10 cm^2. This difficulty is compounded by the fact that fine-grained lithologies are highly weathered, with only the most competent conglomerate and sandstone intervals standing in relief (Figs. 2–4). All finer lithologies, ranging from coarse-and-medium grained lithic wacke to fine mudstone, appear as "powder" on the surface exposures due, in part, to the effects of climate on the presence of smectitic clay. In addition, recent salt deposits spread across bedding planes obscure or obsfucate adpressions, where preserved, and selenite crystals along vertical cracks control where lithologies split in some intervals.

The depth to which weathering has occurred may be up to a meter or more, requiring excavations and trenching to find and sample competent rock. The most easily accessible competent rock occurs at the crests of the piedmont "hills", which may be 1700 m or higher in elevation. In nearly all instances, these lithologies cannot be traced laterally because the adjacent slopes are covered in deeper, weathered overburden. It is only possible to excavate pits of approximately 50–150 cm, or so, in width before attempting to "delaminate" an interval from bottom to top, exposing plant debris. The Sisyphus effect also hinders recovery. As deep pits or trenches are excavated, adjacent weathered debris continuously fills the hole, doubling or tripling the time to recover the centimeter-sized fragmentary fossils. Hence, there is a very restricted surface area of any fossiliferous bed with which to evaluate assemblages, and limitations on tracing and sampling beds along strike hinder attempts at determining what lateral relationships may exist in the deposit.

Permineralized wood is more common than permineralized rootlets. Silicified wood occurs mainly in fluvial channel-lag deposits ranging from coarse conglomerate to coarse-grained sandstone, and is unaffected by either tectonism or recent weathering. *In situ*, silicified trunks with attached rooting in paleosols are uncommon. The systematics of many of these wood assemblages have been published by Wan et al. (2014, 2017,

2021a). In addition to permineralized roots attached to upright trunks, one stratigraphic interval in South Taodonggou preserves both *in situ*, vertically oriented and non-oriented, permineralized rooting structures in sandy coarse siltstone (Wan et al. 2019a). The localities from which these reports originate also were visited during field work.

Due to the nature of adpression assemblages, field images were supplemented, where possible, with subsequent re-imaging of hand samples returned to the Nanjing Institute of Geology and Palaeontology. This small sampling of adpressions is housed in the paleobotany collections. Unfortunately, when adpressions were recovered and returned to Nanjing from previous field excursions, the city's humidity interacts with the shrinking-and-swelling smectite-clay minerals during storage, reducing the fine-grained lithologies to powder and eliminating their utility. Hence, it is emphasized that the following results and discussion are based on limited materials as observed in the field.

Assessment of Taphonomic Assemblage Occurrences

The localities reported by Yang et al. (2021) used in this study were described at centimeter scale over a 20-year period. The Wutonggou–Jiucaiyuan–Shaofanggou succession totals 4709 m of measured stratigraphy (Yang et al. 2010, 2021; Fig. 1). These three LCs are subdivided into 1838 high order cycles (HC), which are defined on the basis of repetitive changes of sedimentary environments. The presence and taphonomic character of plant assemblages in each HC, the depositional setting assigned to the HC, and their occurrences (see Yang et al. 2021, supplemental data) were compiled to evaluate their spatial and temporal distribution in the upper Permian and Lower Triassic. Paleobotanical assemblages are first evaluated according to the type of plant part recorded at the time each section was measured. The four assemblage categories are: (1) permineralized, coalified wood or wood impressions; (2) adpressions that can be identified either to plant part (axis, leaf, pinnule, reproductive organ) or systematic affinity (fern, horsetail, lycopsid, gymnosperm); (3) phytoclasts consisting of fragmentary plant parts, generally $\leq$ 1 cm^2 in surface area (recorded as "large" in field notes), and unable to be assigned to any systematic group; and (4) rooting, identified as carbon films, rootlets, root halos, root molds, calcite-filled tubules, and rhizoconcretions. Adpressions and phytoclasts were further described in the field with the categories: (1) identifiable (woody or permineralized, charcoal, delicate, or leaf imprint) remains that represent axial or leaf remains; (2) abundant/rich/concentrated, where a heteromeric (clasts of various sizes; Gastaldo 1994) phytodebris assemblage preserves clasts up to 10 cm in one dimension but, generally, consist of several HC bedding planes that are covered in meso- (1 cm^2) to microfossil (mm^2) debris; (3) common, where bedding surfaces are draped in organic debris, with individual phytoclasts not in contact with neighbors; (4) some (sparse, scattered, rare), where there are isolated or dispersed phytoclasts on bedding; and (5) disseminated (dispersed, tiny, minute), where an isomeric (all phytoclasts of similar size; Gastaldo 1994) assemblage consists of millimeter-sized organic particles that drape bedding planes. A subset of six stratigraphic sections, totaling 3247 m, was evaluated to understand the proportional distribution of phytoclast categories in each LC and their occurrence across the study area. Phytoclast occurrences in an individual HC were scored based on descriptions of individual beds, horizons, lithologies, or intervals observed, therein. Data worksheets are available in the Online Supplemental File.

RESULTS

Taodonggou and Tarlong

Taphonomic Assemblages.—Fossil-plant assemblages in Tarlonggou and Tarlong consist of: (1) *in situ*, autochthonous standing permineralized gymnosperm axes (e.g., Wan et al. 2019a); (2) rare, bedded parautochthonous adpression assemblages in mudstone underlying organic-rich coaly shale and coal; (3) allochthonous (transported) assemblages of dispersed logs, also permineralized, in extraformational and intraformational conglomerate; (4) rare compression/impression transported assemblages in which identifiable leaf taxa are preserved in lenticular fluvial deposits; and, most commonly, (5) transported phytoclasts, some of which may be identifiable to major plant group (e.g., sphenopsid, fern, gymnosperm), as drapes on upper bounding surfaces of fining up beds in both fluvial and limnic deposits.

Autochthonous Permineralized Assemblages.—To date, two horizons have been found where *in situ*, erect permineralized basal trunks and their root systems are preserved and exposed along strike. One interval occurs in Wuchiapingian deposits cropping out in South Tarlong (Fig. 5; N45.2531°, E089.0489°). The other is found in South Taodonggou (Fig. 6; N43.2319°, E088.9733°) where it is closely associated with the age-modeled PTB (Yang et al. 2021). Both are in the Wutonggou LC (Fig. 1); the former is placed in the Wutonggou Formation and the latter in the overlying Guodikeng Formation.

The Wuchiapingian forest transect consists of 39 basal stumps, attaining diameters of $\sim$ 60 cm, that are rooted in a light olive-gray, poorly sorted wacke (Fig. 5A). Permineralized bases with coalified rooting systems occur along strike (based on excavation). These large trees possess distinct growth rings which may, in fact, be false growth rings (unpublished data) and are assigned to *Protophyllocladoxylon*. The trees are buried in a lithic wacke in which fragmentary axes, degraded detritus, and charcoalified megafossils are preserved. An olive gray siltstone of $\sim$ 5 cm in thickness is exposed in the section and overlies one entombed tree. Here, a concentrated adpression assemblage of axial remains and pinnae assigned to *Callipteris* sp. (Fig. 5B–5D) is preserved. In other cases, degraded and fragmentary macro- and mesofloral remains occur as bedding drapes, none of which can be assigned systematically.

Erect, permineralized Early Triassic tree stumps in the uppermost Wutonggou LC are confined to one or possibly two (due to a fault offset to the southeast) closely spaced horizons along strike (108°) for a distance of 265 m at Taodonggou (Fig. 6A; N43.2319°, E088.9733°; Wan et al. 2019a). Trees are exposed in vertical relief on the northern side of the valley (Fig. 6A) and a group of nine are exposed in plan view in a dip slope through which they project. These nine trunks occur over an area of 128 m^2, range in diameter from 6–15 cm, and are variously preserved. All trunks are inclined relative to vertical, with a prevailing (present day) northeasterly direction. Cellular preservation, in general, is very good and growth rings are absent. At least one trunk exhibits interior rot prior to silicification and compaction, resulting in the distortion of the basal part of this particular tree upon compaction of entombing sediment. The wood consists of tracheids with araucarian-type pitting and rays with one to two large, simple pits in each cross-field; this wood is assigned to *Zhuotingoxylon* (Wan et al. 2021a). Rooting structures are not permineralized, but are coalified and compressed (Fig. 6C) in a medium dark gray coarse siltstone with dispersed medium sand grains. Small, coalified axes and degraded plant debris occur at the interface of the paleosol and overlying sediment.

Specimens of *Zhuotingoxylon* are preserved to heights of at least 1.45 m along the northern exposure and up to 60 cm on the opposite side of the valley (Fig. 6B). Trunks are entombed in an olive-gray, sandy coarse siltstone that fines up to mudstone with a minor silt component. Trunks and rooting are buried by two cross-bed sets, both of which exhibit vegetation-induced sedimentary structures (Rygel et al. 2004). The basal bedset is at least 40 cm in thickness and consists of upturned cross-beds that cover $\sim$ 20 cm of trunk length on both sides of the tree. A horizontal surface separates the basal from the upper bedset. The upper bedset consists of well-developed planar cross beds at a moderate angle, the geometry of which changes to trough cross bedding once the beds

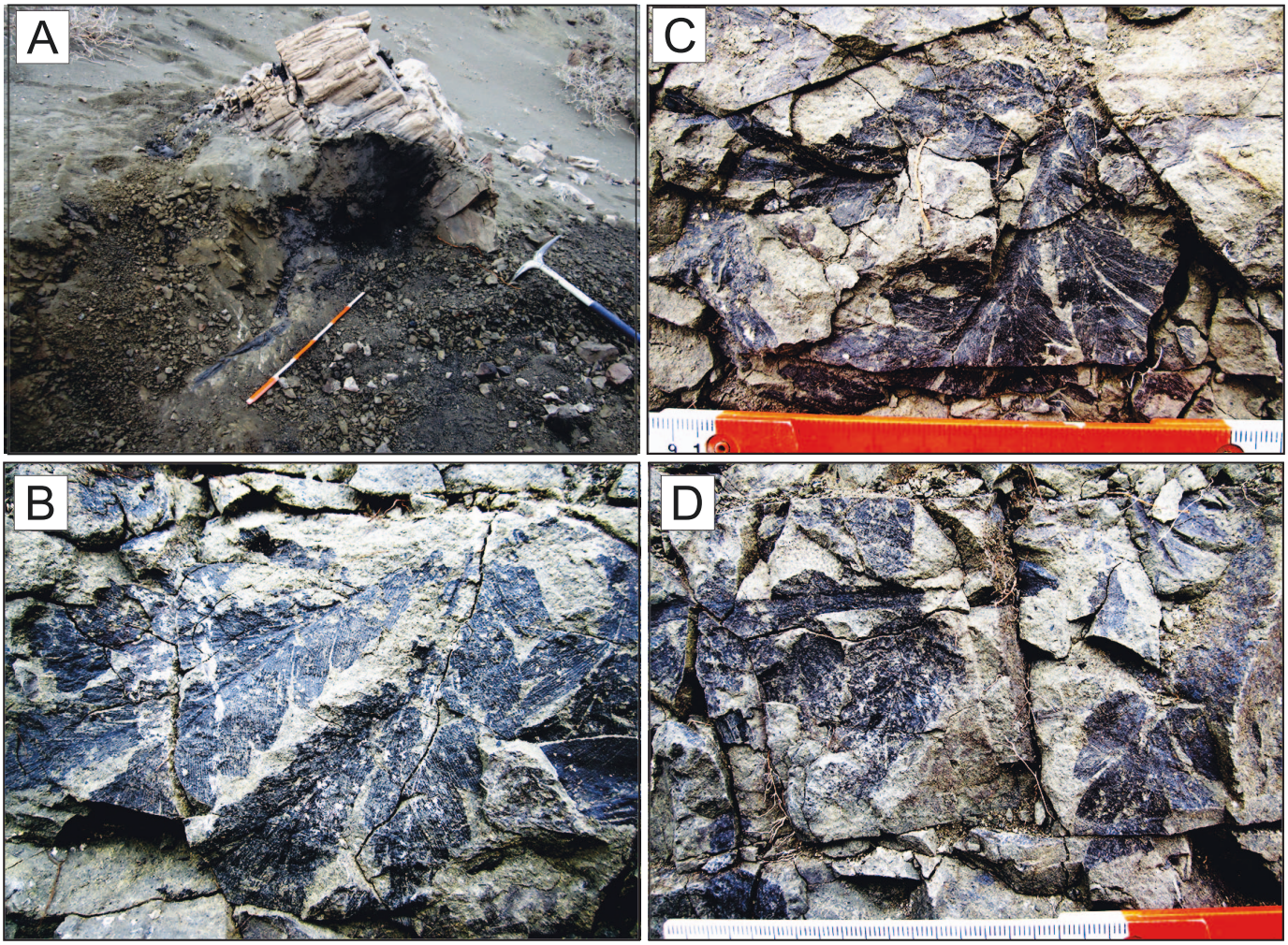

FIG. 5.—Erect, permineralized trunks and overlying adpression assemblage of Wuchiapingian age, North Tarlong (N43.2531°, E089.0489°). **A**) Basal stump of *Protophyllocladoxylon* (Wan et al. 2019a) and rooting entombed in a paleosol dipping at a moderate angle. Pickaxe and ruler scaled in decimeters. Parautochthonous/allocthonous adpression assemblage in overlying coarse, olive-gray siltstone. **B**–**D**) *Callipteris* sp. cf. *C. adzvensis* Zalessky. Scale in cm and dm.

migrated to and encountered the trunk (Fig. 6B). Hence, erect trunks acted as obstacles to bedload sedimentation evidenced by cross-bed sets lapping against the axis relative to the upstream flow direction and overtopping the trees (Fig. 6B).

Parautochthonous Adpression Assemblages

Two intervals in the lower Wutonggou LC in Central Tarlong (Fig. 2D) preserve adpression assemblages (Fig. 7), one of which is in a transgressive and one in a regressive phase of rift lake expansion and contraction, respectively (Wctd19/20; Yang et al. 2021). Both intervals are associated with organic-rich and thin coal, and fossils occur in medium-dark gray, coarse siltstone that fines upsection. Wctd19 is interpreted to represent prodeltaic deposits, whereas Wctd20 is interpreted as deposits of a lake-margin setting. In both instances, prostrate axes predominate in the coarser intervals over which are well-preserved leaf-bearing assemblages. Terminal pinnules/pinnae were disarticulated from larger fronds and are common in the limited volume of rock assessed (Fig. 7B–7E). Here, taxa include *Callipteris* (Fig. 7B, 7E), and *Pecopteris* (Fig. 7C, 7D) representing suspension-load settling to the bedload interface.

One organic-rich/coal interval, Wstr 177 (Yang et al. 2021) in the upper Wutonggou LC, is exposed in South Tarlong (Fig. 8). Yang et al. (2021) report an early Changhsingian age of 253.39 ± 0.04 Ma for this cycle at this locality. Here, a heteromeric megafloral assemblage is preserved in mudstone associated with this facies. Coalified plant remains and bedding surfaces appear shiny and polished, the consequence of tectonic deformation and bed shearing. Due to the combination of a moderate dip (41°), calcite-fracture fills, and the depth of surficial weathering, it is not possible to assess the extent and orientation of plant-debris coverage on many bedding surfaces (Fig. 8C). Where some confidence can be placed on this taphonomic assemblage, calamitean axes and those of undetermined affinity appear to be oriented randomly, and these concentrated in low-angle, trough cross-beds. Articulated *Asterophyllites* (Fig. 8B) and leaves conforming to *Cordaites* (Fig. 8D) accompany the axial-dominated assemblage, although the majority of bounding surfaces of bedding exhibit degraded phytodebris with cuticles (Fig. 8B).

Allochthonous Permineralized Assemblages.—Isolated permineralized logs (Fig. 9A) and log assemblages occur more commonly throughout the upper Permian–Lower Triassic succession than any other type of plant assemblage, except for unidentifiable, comminuted phytodebris (see below). Woody debris occurs in basal lags of both clast- and matrix-supported, cobble-pebble-granule conglomerate and coarse- to medium-grained, sandstone channel-fill deposits. Silicification

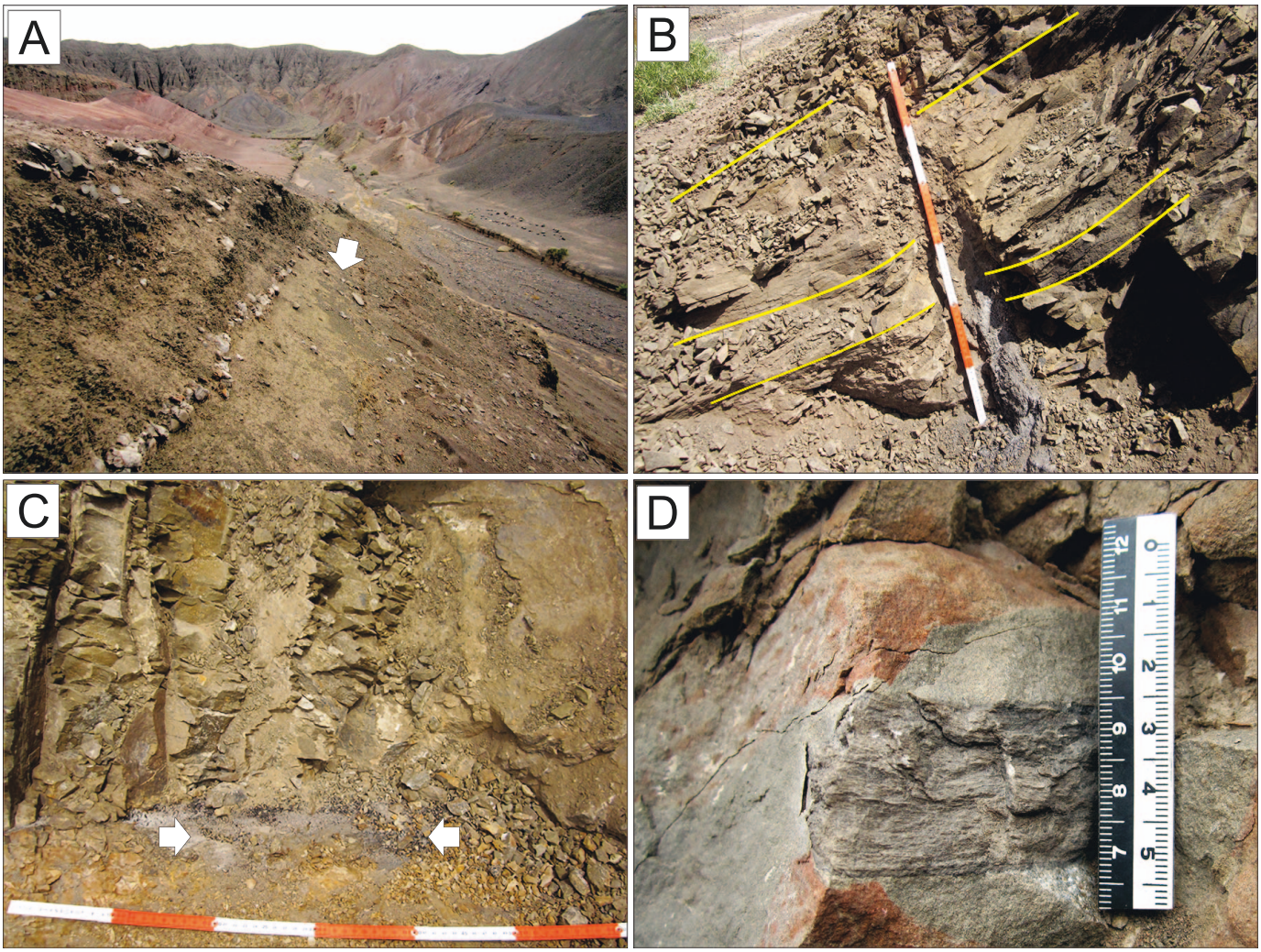

FIG. 6.—Erect, permineralized trunks in Taodonggou assigned to *Zhuotingoxylon* (Wan et al. 2021) of earliest Triassic age; estimate based on regional age model of Yang et al. (2021; N43.2308°, E088.9769°). **A**) Paleosol horizon (white arrow) in which trunks are rooted and project from the exposure; erect trees can be traced for ~ 300 m along strike. **B**) Erect, small diameter trunk entombed in an olive-gray, sandy coarse siltstone where cross-beds (yellow lines) lap against the upstream side of the trunk, having displaced it from vertical by ~ 35°. Cross-beds (yellow lines) on the downstream side show little distortion. **C**) Coalified rooting structure in a sandy, coarse siltstone, undifferentiated paleosol (white arrows). **D**) Permineralized woody root (e.g., Wan et al. 2019b). Scales in cm and dm.

enhances the probability that these fossils will remain exposed on weathered surfaces, although samples are prone to fracture and displacement (Fig. 9C). Permineralized transported logs have been reported from the lower (Wan et al. 2014) and upper (Wan et al. 2021a) Wutonggou, Jiucaiyuan (Wan et al. 2019b), and the Shaofanggou LCs. Their frequency of occurrence is very low relative to available stratigraphic thickness (see below).

One distinctive assemblage (Fig. 9A) is exposed on a dip slope of a poorly sorted, extraformational conglomerate, interpreted as an anabranching system. The assemblage consists of more than 100 logs ranging in diameter from a decimeter to nearly 50 cm distributed across the outcrop surface. Due to the dip angle and accessibility, it is not possible to determine whether these represent an actual log jam or a large woody debris field associated with one or more barforms. Confirmation of their arrangement requires a 3D survey of the log distribution and orientation, relative to the underlying conglomerate, which would be facilitated with drone imagery. Unfortunately, the use of private drones in Xinjiang Province is prohibited.

Allochthonous Adpression Assemblages.—Allochthonous debris, similar to the meso-detritus in other parts of the basin, is the most commonly preserved plant parts. These occur as drapes in trough cross-bed laminae, and scattered in condensed intervals of rift-basin lake systems (as identified by shell accumulations of concostrachans). Organic matter drapes are associated with muscovite flakes, indicating their hydrodynamic equivalence.

Daolongkou
Taphonomic Assemblages

Allochthonous Adpression Assemblages.—Fossil-plant assemblages in Daolongkou consist of transported (allochthonous) plant parts (Figs. 10–12). Their occurrence is sporadic and the extent to which any lenticular or bedded assemblage can be traced is, at best, a few meters laterally. This limitation is due to bed attitude and weathering constraints that are more extreme than rocks in Tarlongguo and Tarlong. Accessible collections are made at the narrow ridge crests where overburden is minimal (< 0.5 m), but the high-angle dip of beds, again, constrains the size of rock fragments

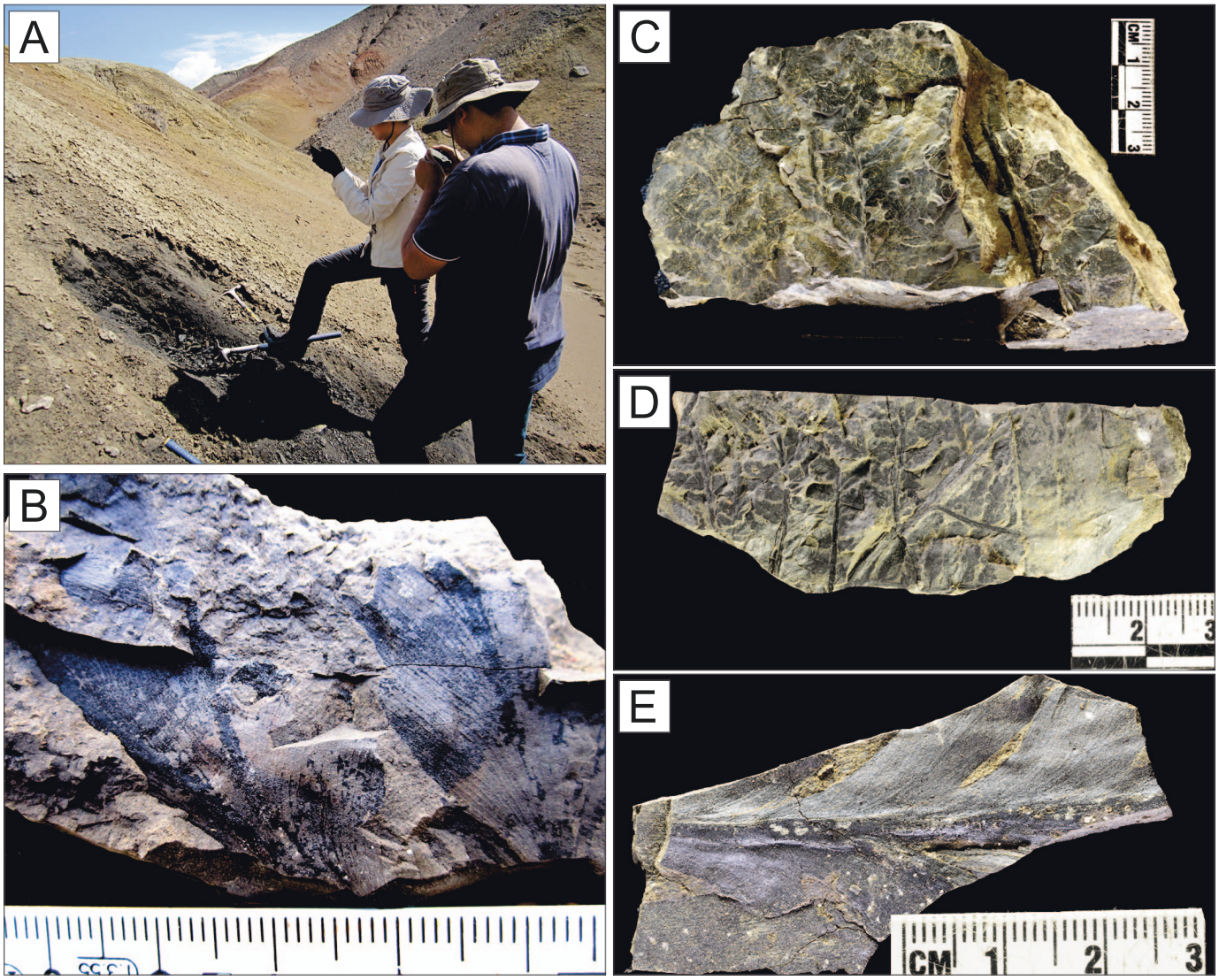

FIG. 7.—Late Permian (?), rift-lake deposits in Central Tarlong (N43.2528°, E088.9695°). **A**) Brown-gray to olive-gray mudstone in which a thin interval of bedded allocthonous leaf fragments are preserved. **B**) Fragmentary specimen of *Callipteris* in which venation is well preserved. **C**, **D**) Fragmentary specimens of penultimate and ultimate rachises bearing pinnules assigned to *Pecopteris*/*Sphenopteris*. **E**) Fragmentary specimen of *Callipteris* pinnules. Scales in cm and mm.

that can be recovered (Fig. 10A). Two generalities can be made, although these are based on a limited number of sampling sites mainly in the lower part of the Wutonggou Formation (Changhsingian). Large plant remains, in the sense of 0.5 m-scale leaf parts (some order of rachis with lateral pinnae attached, collected in numerous pieces to reconstruct the size of the fossil), occur in fluvial sandstone either in basal channel deposits of sandy coarse siltstone or in sandy siltstone trough fills (as determined by small-scale, low-angle trough cross-bedded sandstone). Our 2019 collection in South Daolongkou consists mainly of pinnae that appear to be assigned to the pteridosperm *Callipteris*, or a plant with a similar leaf morphotype (Fig. 10C). These specimens are accompanied, and dominated, by assemblages of leaves in which parallel venation is preserved (Fig. 10D). Most plants are concentrated on bedding planes as organic drapes in various states of preservation (Figs. 10B). All poorly preserved assemblages, some with charcoal, overlie the thin intervals in which the larger leaves occur. Mud-cast rachial axes are present along with coalified compressions, and permineralized wood, have been reported from the LC (Wan et al. 2017).

Two plant-bearing siltstone intervals in North Dalongkou (N88.8705°, E043.9617°) were sampled; one in the Wutonggou LC (Figs. 11) and the other in the Jiucaiyuan LC (Fig. 12). The Permian assemblage (N43.9621°, E088.8781°) occurs in a short (45 cm) stratigraphic interval of olive-gray coarse siltstone/mudstone dipping at a low (24°) angle. Here, aerial axes occur as adpressions or mudfill casts and leaf debris appear either as coalified compressions or impressions. A thin (5 cm) mudstone in which aerial axes, pinnae, and pinnules of *Callipteris* (Fig. 11B, 11C) and *Noeggerathiopsis* (Fig. 11D) are preserved in fine siltstone. An interval of sandy coarse siltstone overlies the megafloral assemblage where millimeter-scale laminae and cross-laminations are draped in concentrated, dispersed, and comminuted plant debris (Fig. 11B). The second assemblage (N43.9595°, E088.8781°) is Triassic in age and occurs in a fine-to-medium grained, cross-bedded sandstone near the top of the measured section (Yang et al. 2021; Fig. 12). Bedding surfaces are covered in either a heteromeric, fragmented and degraded assemblage of aerial plant parts (Fig. 12B) or larger fragments of axial and pinnae debris associated with mica (Fig. 12C). A thin mudstone contains well-preserved

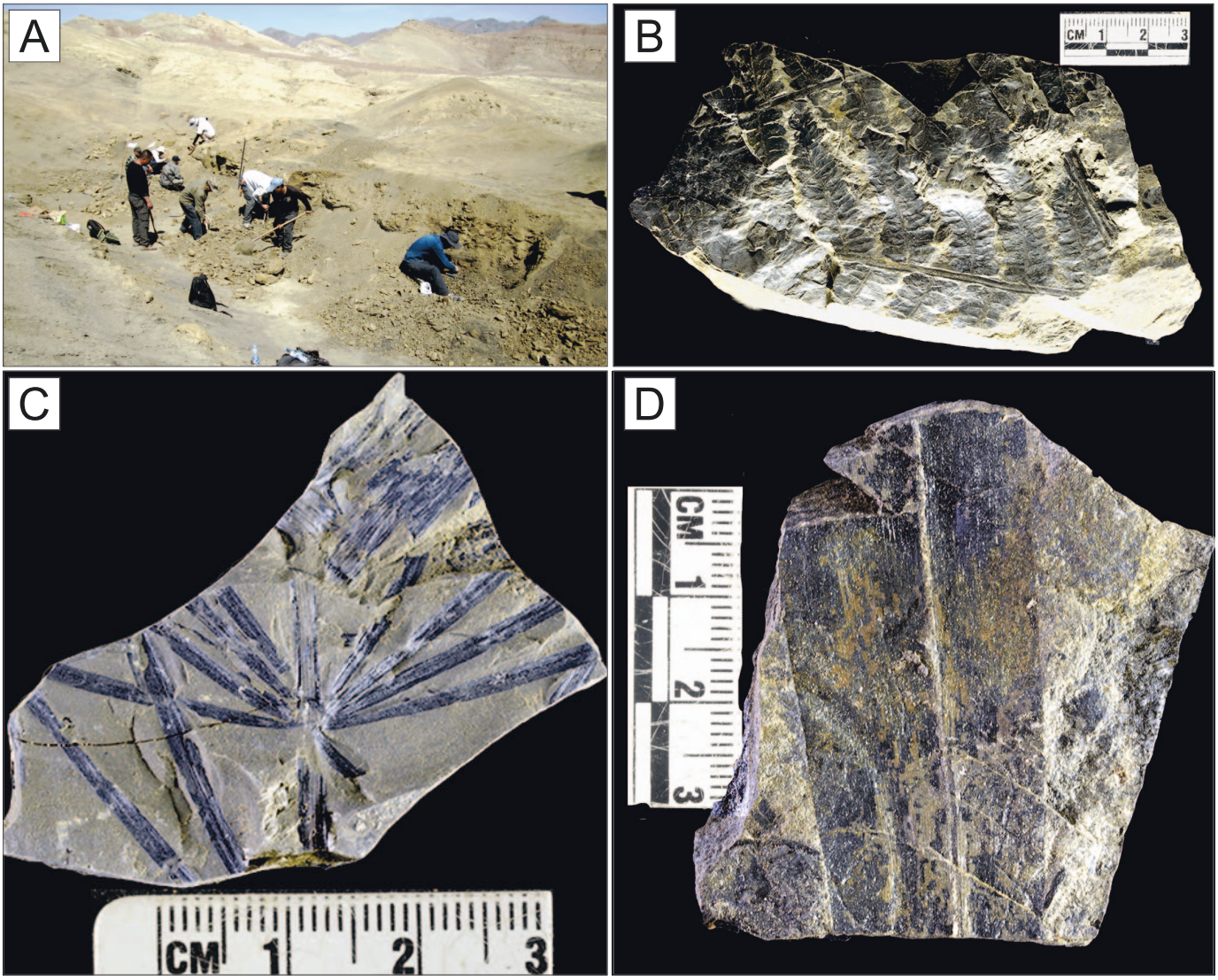

FIG. 8.—Coal-bearing interval in South Tarlong (N43.2597°, E089.0356°). **A**) Olive-gray, fine mudstone in which low-angle, mm-thick, trough cross-beds preserve a parautocthonous/allochthonous plant assemblage above a coal. **B**) Calamitean axis with long *Asterophyllites* leaves. Carbonized remains appear shiny as a consequence of tectonism. **C**) Partial pinna and ultimate pinnules of *Pecopteris*. **D**) Striated, fragmented leaf of cf. *Cordaites*. Scales in cm and mm.

leaves of a thalloid plant (Fig. 12D). We caution, again, that the steep angle of beds combined with deep surficial weathering in all sites precludes extensive trenching and sampling.

Zhaobishan
Taphonomic Assemblages

Allochthonous Permineralized Wood.—Permineralized wood, logs, and fragmented specimens, are the most conspicuous plant fossils in Zhaobishan. Specimens occur in both the uppermost Permian and Triassic (Wan et al. 2019a). Unlike the logs distributed in a conglomerate sandstone in Tarlong, here fossil wood occurs isolated either in the base of, or incorporated in barforms, of lithic wacke sandstone or conglomeratic sandstone bodies (Fig. 9B). When entombed in barforms, specimens were collected from surficial exposures. Axes attain at least 19 cm in diameter in which preservational quality is good to excellent. The degree to which cellular preservation is retained, though, is a function of the degree to which the trunks and branches had decayed prior to silicification.

Allochthonous Adpression Assemblages.—Although adpression assemblages occur in Zhaobishan, these are restricted either to organic drapes atop channel-sandstone bedforms or in shale/siltstone intervals deposited at depth in large rift lakes. Degraded plant parts are associated with conchostrachan assemblages and concentrated in organic-rich shale. To date, very few identifiable megafossils have been encountered and these are limited to herbaceous lycopsid leaves and fern pinnules from the Jiucaiyuan LC. All other assemblages consist of either heteromeric or isomeric debris, associated with muscovite, and concentrated or dispersed on bedding in fluvial deposits.

Phytotaphonomic Occurrences

High-order cycles, distinguished on the basis of repetitive changes of sedimentary environments, vary over space and time in the study area. HCs range in thickness from intervals < 1 m, in which a single lithology or lithological association is present (e.g., fining up), to ones that are > 10 m or more in thickness. In general, thick HCs consist of several lithologies (cobble-pebble conglomerate fining to an array of sandstones and

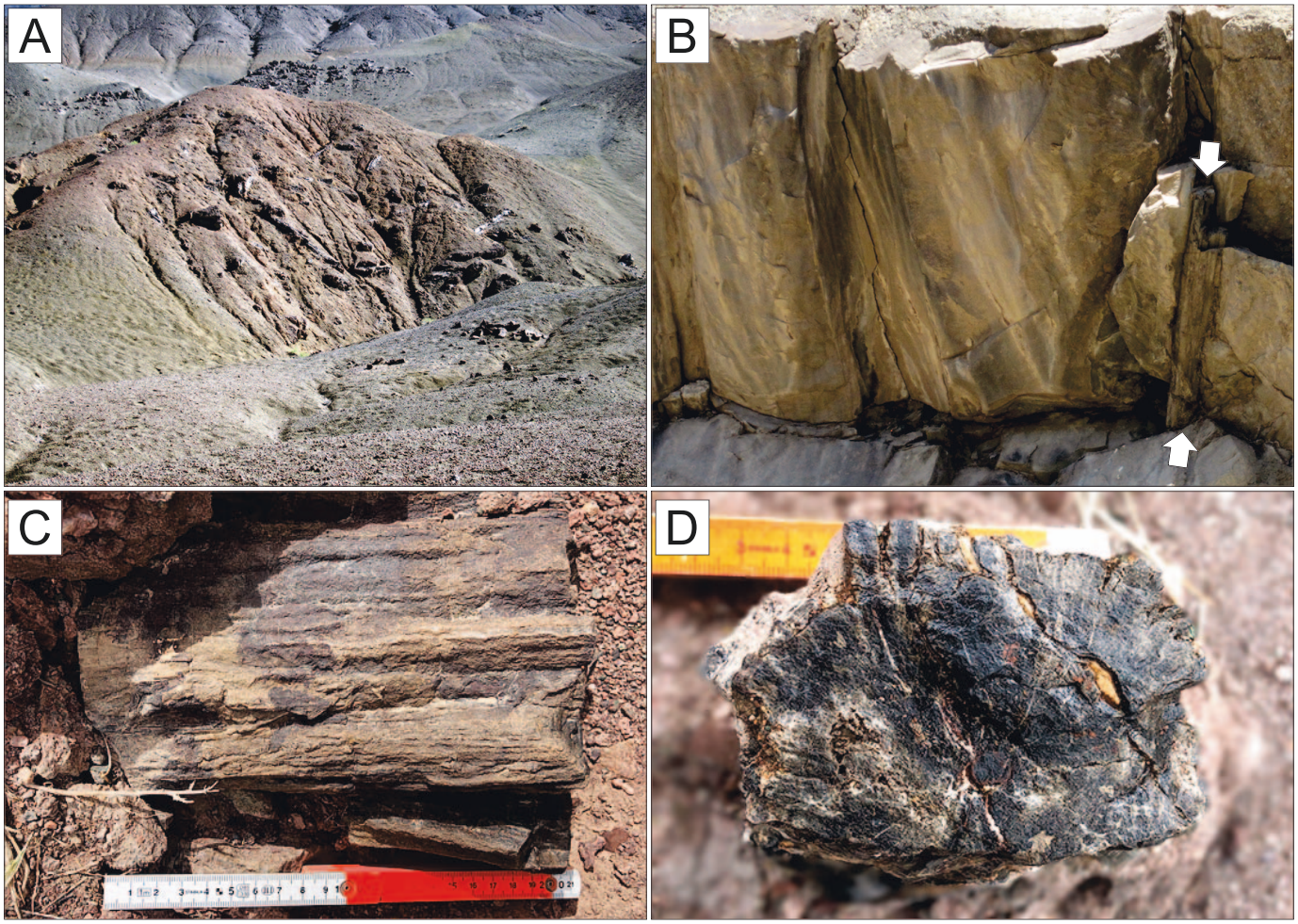

FIG. 9.—Exposures of Permian and Triassic permineralized wood assemblages. **A**) Coarse conglomeratic sandstone with permineralized logs exposed on a high-angle dip slope in North Tarlong (N43.2685°, E089.0509°). The braided river facies is Changhsingian in age. **B**) Isolated log (arrows) at the base of conglomeratic, coarse-grained sandstone channel facies in Zhaobishan (N43.246375°, E090.429025°). **C**) Fragmentary piece of an Early Triassic permineralized wood. **D**) Cross-section of Early Triassic permineralized wood (branch). Scale in dm and cm.

mudstones) that may be organized into repetitive cycles, representing different facies of the same sedimentary system (Yang et al. 2021, supplemental data). Hence, scoring of taphonomic occurrences in any one HC in the following analysis might represent a single horizon or sedimentary structure (e.g., bedding surface(s) on trough cross-beds or bedsets), or multiple horizons or multiple beds in one or more different lithologies.

An evaluation of 1838 Wutonggou–Jiucaiyuan–Shaofanggou HCs shows regularity in the frequency of two plant-assemblage categories, and wide variance in the other two categories. When observations are compiled and compared, permineralized wood and adpression assemblages are found to occur in < 6% of HCs in localities where all three LCs are exposed (Table 1). Where only the Wutonggou LC is exposed and described, wood and adpression categories each comprise < 4% of HCs, in which identifiable plant fossils occur. The proportion of HCs in which phytoclasts are preserved ranges more widely, from 11% (Zhaobishan, N = 484 HCs) to 63% (Dalongkou South, N = 167 HCs). Higher proportions of phytoclasts are reported in SW Tarlong and S Tarlong where only the Wutonggou LC crops out. Similarly, the proportion of HCs in which rooting structures are recorded ranges from a low of 1% (Zhaobishan, N = 484 HCs) to 57% (Dalongkou North and South Taodonggou, N = 70 and N = 129, respectively). In localities where only the Wutonggou LC crops out, the frequency of preserved rooting structures is in the range of 17–28% (Table 1). We note that most paleosols in these fully continental successions do not preserve physical evidence of rooting. This is in spite of extensive pedogenic and geochemical evidence of soil development (Yang et al. 2007, 2010, 2021; Thomas et al. 2011). A different story emerges when each LC is compared across the region.

The Wutonggou LC occurs in each locality. As such, this HC contributes the largest number of observations (N = 1329) to the data set. Yet, regardless of the geographic site of the measured section, the frequency of either permineralized wood or adpression assemblages only represents < 4%. In 11/16 tallies, permineralized wood and adpression assemblages account for < 2% of the record. In contrast, rooting is more common than phytoclasts in all but a few localities (i.e., Dalongkou North, S Taodonggou , N/C Taodonggou). This is a likely a function of the measured section transect and the interception of more paleosols than fluvial or limnic deposits. It is also the case for taphonomic assemblages in both the Jiucaiyuan and Shaofanggou LCs where rooting is calcified and preserved in calcic paleosols (Table 2).

Data for both the Jiucaiyuan and Shaofanggou LCs originate from four localities, spread across the study area from Zhaobishan in the east to Dalongkou and Taodonggou in the west. Phytoclasts are preserved in most HCs in all stratigraphic sections except in the Jiucaiyuan LC measured in C

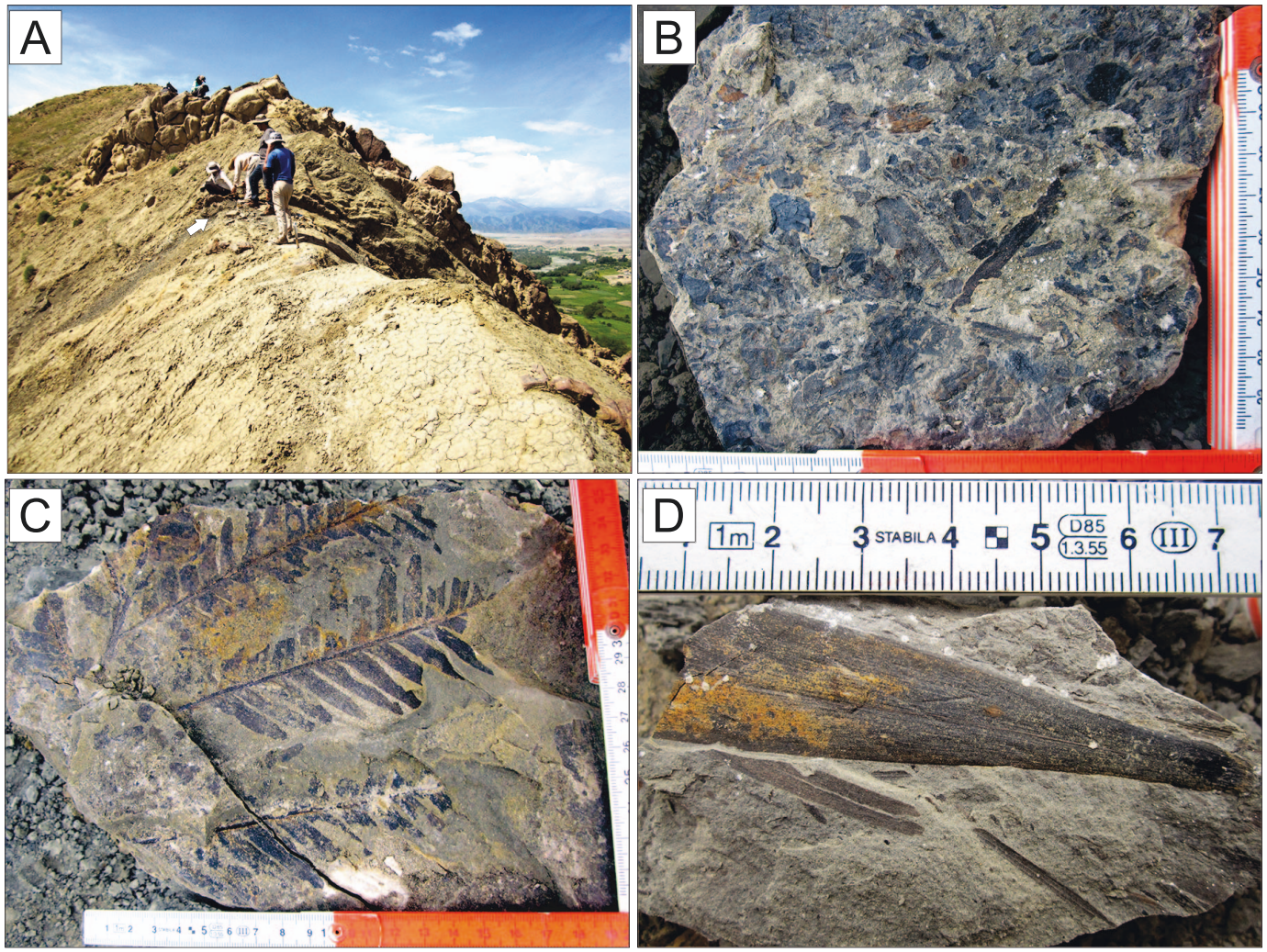

FIG. 10.—Adpression assemblage in Dalongkou South of Wuchiapingian age, Wutonggou LC (N43.26812°, E089.0511°). **A**) Exposure of allochthonous adpression assemblage preserved at the base of a feldspathic wacke at the crest of the Bogda foothills. **B**) Heteromeric, concentrated adpression assemblage of randomly oriented axes, phytoclasts, and (?) charcoal draped across bedding surfaces of cross-bedded sandstone (e.g., Wan et al. 2016, 2021b). **C**) Well-preserved frond fragment and ultimate pinnae of *Callipteris* in basal sandstone trough fill. **D**) Well preserved, striated, partial leaf cf. *Cordaites*. Scales in dm and cm.

Taodonggou. In contrast, rooting structures are preserved in the majority of HCs in all locations except in the Jiucaiyuan LC in Zhaobishan and Shaofanggou LC in Dalongkou South (Table 1). In fact, the rooting structure category is the only one recorded in N/C Taodonggou where it occurs in 90% of the HCs. The absence of the wood, adpression, and phytoclast categories, here, is a function of the facies association(s) encountered in the transect.

In an attempt to understand the occurrence of well-preserved megafloral elements versus the frequency of various transported phytoclast categories, spread over more than 100 km, we present data from 1260 observations taken from 3247 m of stratigraphic section (Table 2). The proportion of megafloral elements recorded as "well preserved" accounts for 11% of observations in a single locality, NE Tarlong, where only 110 m of the Wutonggou LC crops out. In all other locations, the percentage of identifiable megafloral elements accounts for $< 6\%$ of observations. In contrast, phytoclasts are the most common, covering bedding planes in various concentrations in all localities. In any one HC, phytoclasts are slightly more common as drapes than bedding surfaces on which phytoclasts are considered abundant. Both categories, though, occur more frequently than bedding planes described as hosting sparse or disseminated assemblages. Hence, disseminated (comminuted) plant detritus is a persistent feature of more than a third of HCs in the upper Permian and Lower Triassic successions in western China, with a decrease in frequency in the Shaofanggou LC (Table 1).

Relationships between Megafloral Assemblage, Depositional Environment, and Climate

Megafloral occurrences are preserved unequally in the Bogda-graben successions, in which braided streams, meandering fluvial regimes, lacustrine deltaic, and lake plain and littoral deposits are interpreted. Similarly, preservation of different megafloral elements occurred under climatic conditions that ranged from arid-semiarid to semi-humid/humid (Table 3). We emphasize, again, that the number of beds, horizons, or intervals in which megafloral elements are found to be preserved is a function of several interrelated factors. These include sediment type, rate of sedimentation in any particular regime at any point in time, geochemical variations in space and time, and paleogeography.

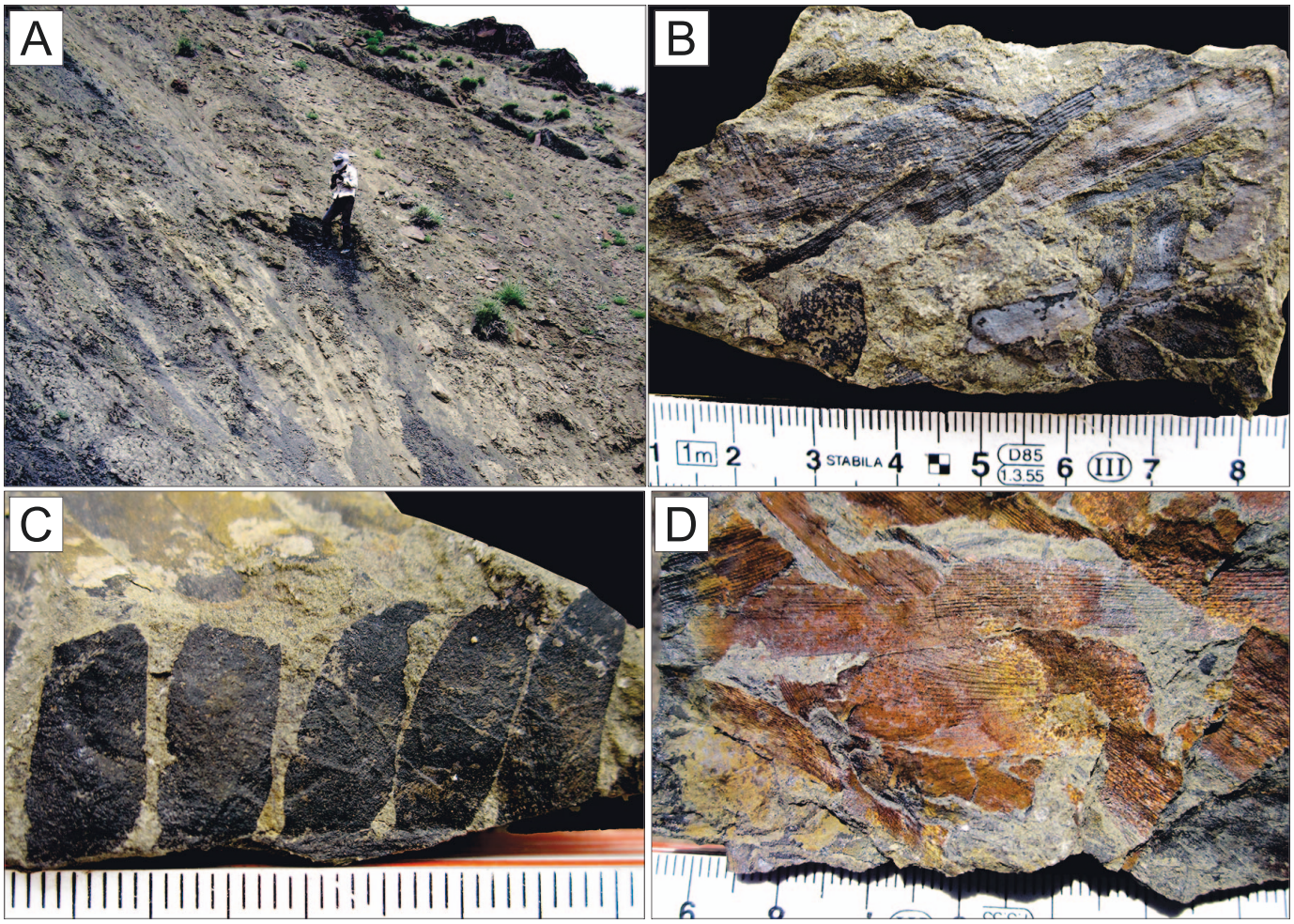

FIG. 11.—Allochthonous adpression assemblage in Dalongkou North of Changhsingian age, Wutonggou LC (N88.8705°, E043.9617°). **A**) Exposure of olive-gray fine mudstone in which a parautochthonous/allochthonous fossiliferous interval is preserved in mm-scale bedding. **B**) Striated calamitean axes and fragmentary pinnule cf. *Callipteris*. **C**) Ultimate *Callipteris* pinnae with five pinnules. **D**) Iron-stained impressions of *Noeggerathiopsis*. Scale in cm and mm.

Coarse woody debris (Gastaldo 1994), either coalified or permineralized, is encountered in each of the broad depositional settings and across the climate spectrum. The rank-order occurrence of woody debris indicates that these plant parts are most common in meandering fluvial (50%) and littoral-sublittoral lake (28%) deposits. Woody debris is less common in HCs that include deltaic environments (16%), and only preserved in braided stream deposits in Zhaobishan (6%). Regardless of environment of deposition (EOD), preservation of these assemblages occurred under a semi-humid to humid climate (69%) at nearly all localities. The exceptions occur in South and Central/North Tadongguo where assemblages occur in HCs assigned arid to semi-arid and semi-arid to semi-humid climate regime. We note, though, that the EOD in which all woody debris is preserved is aquatic.

In contrast, adpression assemblages are preserved most often in littoral and sublittoral lake (52%) and deltaic environment (29%) sediments. There is limited evidence for their preservation in meandering river deposits (14%), and we have not encountered a single adpression assemblage in a braided stream landscape (Table 3). The prevailing climate under which adpressions were preserved parallels that of woody debris. Well preserved and identifiable megafloral elements are encountered in HCs developed under semi-humid to humid conditions (67%) at all localities. It is only at the Dalongkou sites that adpressions occur within sediments deposited under a semi-arid to semi-humid regime.

DISCUSSION

The stratigraphic record of plants is notoriously dependent on many factors that play independent roles in their preservation and subsequent recovery. The absence of identifiable plant debris in any depositional system is a function of one or multiple interrelated factors, all of which affect the preservation potential via various biochemic, geochemic, sedimentologic, and tectonic processes over space and time (Behrensmeyer et al. 2000; DiMichele and Gastaldo 2008; Gastaldo and Demko 2011). It is well documented that wetlands have the highest probability of being represented and dominate the Phanerozoic plant record (Wing and DiMichele 1995; Greb et al. 2006, 2022). As such, megafloral preservation in deep time is biased towards coastal (lowland) sedimentary regimes where both accommodation and rates of sedimentation are highest (Behrensmeyer and Hook 1992). In contrast, fully continental (interior) sedimentary systems possess inherent biases that inhibit or prevent plant-part preservation. These biases include, but are not limited to: (1) the small geographical area of fluvial-and-lacustrine depositional systems in which bio/geochemic, hydraulic, and hydrologic conditions might impede decay and promote preservation; (2) the large geographic area over which organic matter recycles in soils, of various pedogenic families, controlled by climate and regional hydrology; (3) the fact that both aggradational and degradational processes operate over regional, basinal, and continental

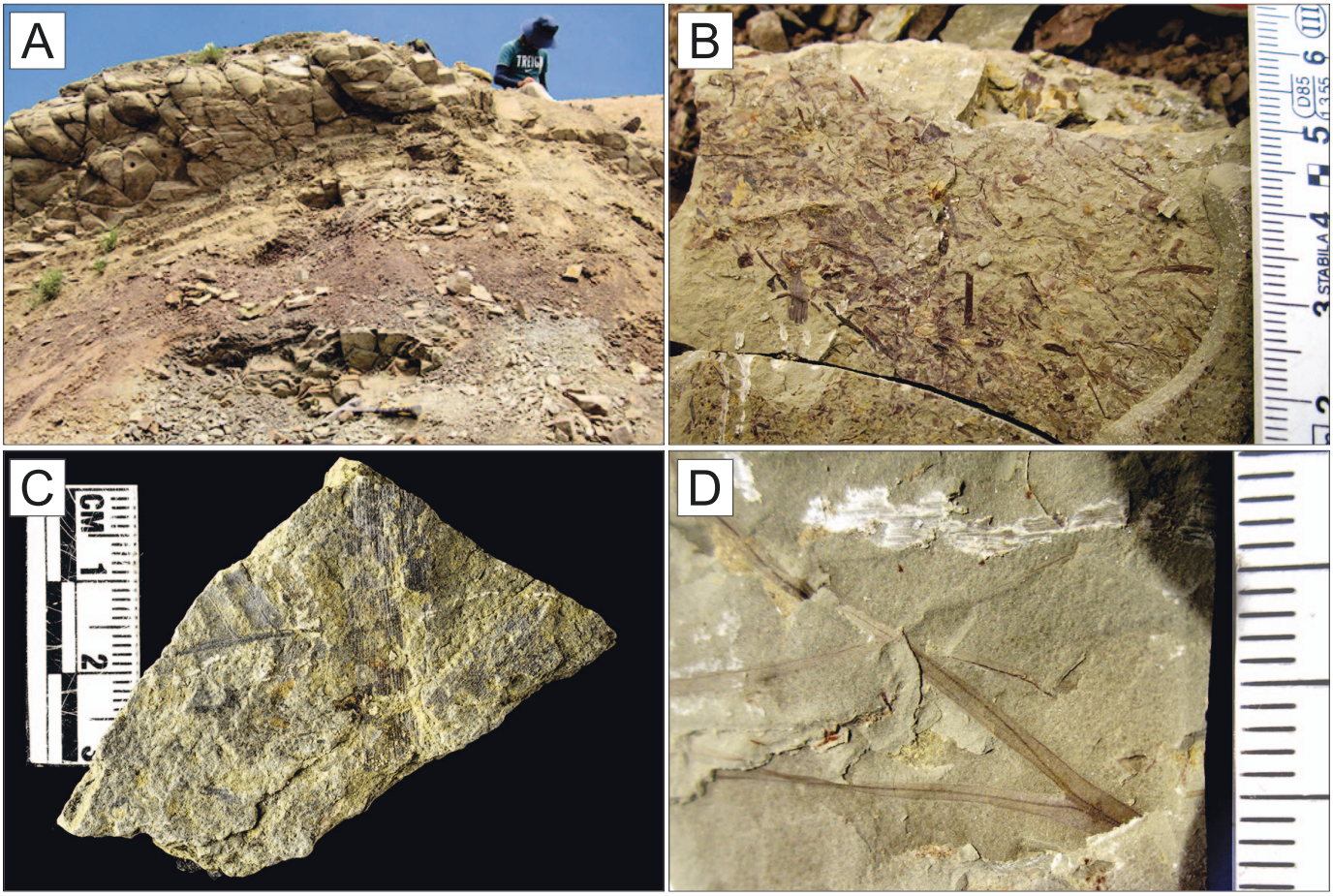

FIG. 12.—Allochthonous adpression assemblage in Dalongkou North of Induan age, Juicaiyuan LC (N43.9595°, E088.8781°). **A**) Dispersed axes and isolated leaves are preserved in an olive-gray fine mudstone and fissile fine-grained sandstone. **B**) Concentrated, mesofossil assemblage consisting of fragmentary axes, leaf impressions, and ?seeds in an olive-gray fine-grained sandstone. **C**) Striated equisetalean axis and poorly preserved, unidentifiable pinnules preserved on bedding in a fine-grained sandstone. **D**) Leaves interpreted to represent a thalloid plant. Scale in cm and mm.

scales, and are influenced to varying degrees in time by both climate oscillations and tectonic activity (Gastaldo and Demko 2011; Gastaldo et al. 2020); and (4) parautochonous-and-allochthonous assemblage composition, diversity, and systematics mirror riparian plants growing along the margins of waterways rather than representing a sampling of interfluvial (floodplain) vegetational diversity (Gastaldo et al. 1987; Gastaldo 1988, 1989; Burnham 1990; Ricardi-Branco et al. 2020). Hence, fossil-plant assemblages in fully continental successions, such as the Bogda Mountains, represent small and very limited "windows" into vegetation at any specific point in time during which these Permian–Triassic landscapes existed (Gastaldo et al. 2005). This contrasts with coastal megafloral records, particularly in the Mississippian (e.g., Gastaldo et al. 2009), Pennsylvanian (e.g., Montañez et al. 2016), and early Permian (e.g., DiMichele et al. 2020), from which long-term biodiversity and ecological trends in stability, turnover, extirpation, and extinction can be discerned with greater confidence. But, the question remains about the actual potential to encounter megafloral assemblages in this stratigraphic record.

Raup (1972), focusing on marine invertebrates, argued that the variation in the area of exposed sedimentary rock per geologic interval is a megabias influencing the evaluation of fossil assemblages. In other words, he maintained that the more rock available to sample resulted in a higher number of taxa that could be recovered which, in turn, affects the interpretation of temporal trends. Since then, his paradigm has been tested both in the marine (e.g., Miller and Foote 1996) and continental fossil records (e.g., Wall et al. 2011). Phanerozoic sedimentary rocks are calculated to comprise ~ 27% marine carbonate, 45% marine terrigenous clastics, and ~ 28% continental terrigenous clastic settings, many of the latter represent coastal plains (Wall et al. 2009). Of the terrigenous clastic settings, Wall et al. (2011) estimate that Miocene (20%), Pliocene (21%), and Cretaceous (27%) rocks comprise the majority of global outcrop area, whereas the total outcrop area for the Upper Permian (Guadalupian–Lopingian) and Lower Triassic equal ~ 800,000 km^2 (5.5%) and 450,000 km^2 (3%), respectively. Hence, when combined with the biases inherent in both the depositional environments in which plant parts may be preserved (Behrensmeyer and Hook 1992) and the unique set of criteria that must be met to finalize its transfer to the lithosphere (DiMichele and Gastaldo 2008), the probability of encountering deep time, fully continental, well-preserved, megafloral assemblages in which systematic identifications can be made remains very low. As Wall et al. (2011) note, outcrop area in continental rock acts as a large-scale bias, largely obscuring the terrestrial diversity signal. This, in part, is likely due to the limited number of depositional settings in which preservation is promoted when compared with the overall vegetated landscape that prevailed at any moment in time.

The high-resolution, litho- and geochronologically correlated Bogda stratigraphies, spanning the end-Permian event and spread across nearly 100 km, offer insight into similar studies where interpretations of vegetational trends are based on one or a few widely separated sections. This is especially true in basins where intense tectonism has affected not

TABLE 1.—*The total stratigraphic thickness of the Wutonggou, Jiucaiyan, and Shaofanggou low-order cycles (LC) along with the number of high-order cycles (HC) recognized by Yang et al. (2021) in each locality. The number of plant taphonomic assemblages recorded in HCs during section measurement, their percent occurrence in their respective LC, the percent occurrence in the cumulative data set for upper Permian and lower Triassic successions. Abbreviations: D_North = Dalongkou North; D_South = Dalongkou South; Zhaob = Zhaobishan; S_TDG = South Taodonggou; N/C TDG = North Central Taodonggou; SW Tarl = Southwest Tarlong; S Tarl = South Tarlong; N Tarl = North Tarlong; NE Tarl = Northeast Tarlong. See Figures 2–4 for locations of measured sections. See text for details; raw data available in Online Supplemental File.*

	D_North		D_South		Zhaob		S_TDG		N/C TDG		SW Tarl		S Tarl		N Tarl		NE Tarl		Total Strat
Section Thickness (m)	308		413		1145		282		457		296		872		826		110		4709
Shaofangguo HO Cycles	27		11		95		42		71										246
Shaofangguo w/perm. wood	1	4%	0	0%	1	1%	1	2%	4	6%									
Shaofangguo w/adpression	0	0%	2	18%	0	0%	0	0%	0	0%									
Shaofangguo w/phytoclasts	2	7%	2	18%	2	2%	5	12%	4	6%									
Shaofangguo w/rooting	12	44%	0	0%	5	5%	19	45%	52	73%									
Jiucaiyuan HO Cycles	27		34		141		26		10				14						252
Jiucaiyuan w/perm. wood	0	0%	0	0%	0	0%	1	4%	0	0%			0	0%					
Jiucaiyuan w/adpression	3	11%	1	3%	0	0%	0	0%	0	0%			1	7%					
Jiucaiyuan w/phytoclasts	12	44%	21	62%	10	7%	2	8%	0	0%			10	71%					
Jiucaiyuan w/rooting	25	93%	6	18%	0	0%	20	77%	9	90%			3	21%					
Wuotongguo HO Cycles	6		122		248		50		128		85		314		318		58		1329
Wuotongguo w/perm. wood	0	0%	4	3%	4	2%	3	6%	1	1%	3	4%	2	1%	3	1%	3	5%	
Wuotongguo w/adpression	0	0%	2	2%	0	0%	1	2%	1	1%	1	1%	1	0%	5	2%	0	0%	
Wuotongguo w/phytoclasts	6	100%	82	67%	43	17%	34	68%	48	38%	62	73%	232	74%	178	56%	34	59%	
Wuotongguo w/rooting	2	33%	68	56%	0	0%	35	70%	3	2%	15	18%	78	25%	54	17%	16	28%	
High Order Cycles	60		167		484		129		209		85		328		318		58		1838
Cycles w/perm. wood	4	7%	4	2%	5	1%	5	4%	3	1%	3	4%	2	1%	3	1%	3	5%	
Cycles w/adpression	4	7%	5	3%	0	0%	1	1%	1	0%	1	1%	2	1%	5	2%	0	0%	
Cycles w/phytoclasts	24	40%	105	63%	55	11%	41	32%	52	25%	62	73%	242	74%	178	56%	34	59%	
Cycles w/rooting	40	67%	74	44%	5	1%	74	57%	64	31%	15	18%	81	25%	54	17%	16	28%	

only the attitude and subsequent weathering of the beds, but also the structural relationships where duplicate or repeated stratigraphies may occur (e.g., Borquin et al. 2018). It is apparent from our data that well-preserved assemblages in all LCs vary across the basin, having been controlled by sedimentary facies, prevailing climate, and geochemical conditions either at the time of burial or processes that operated later in their geologic history (Tables 1, 3; Fig. 13). We also must acknowledge that: (1) the plant-fossil record in the Bogda Mountains reported, herein, is a function of where our sections were measured (selected based on degree and quality of exposure) and (2) laterally equivalent rocks exposed over distances of several hundred to thousands of meters may preserve records that were not sampled. Both of these factors are often unstated and overlooked, but must be acknowledged as a reality in all end-Permian (and other) studies.

Adpression and Phytoclast Trends

Based on adpression assemblages, alone, one might interpret widespread extirpation or extinction of vegetation of these latest Permian and earliest Triassic successions. This interpretation could be justified either based on the absence of adpression assemblages in the record or a difference in their systematic affinities when (infrequently) encountered. In the Bogda Mountains, adpression assemblages are found in $< 4\%$ of HCs. Theoretically, if each adpression assemblage were preserved throughout 1 m of section, these fossiliferous intervals would represent a mere 0.0051% of the rock record. In most cases, though, identifiable assemblages are limited to intervals of a few centimeters to decimeters; reducing the preservation interval to 0.1 m of section decreases this figure to 0.00051%. These occurrences parallel actualistic plant-taphonomic studies of fluvial barforms (e.g., Scheihing and Pfefferkorn 1984; Staub and Gastaldo 2003),

TABLE 2.—*A selected subset of 3247 m of six measured sections, distributed across 100 km of the basin, used to determine the proportion of adpression versus phytoclast assemblages in HCs spanning the Permian–Triassic boundary. See text for details; raw data available in Online Supplemental File.*

	StratThick	TotalObserv	Well Preserved	Abundant/Rich	Common	Sparse	Disseminated	
Dalong South	413	229	6%	32%	32%	20%	10%	100%
Zhaobishan	1145	81	6%	27%	42%	20%	5%	100%
N/C TDG	457	154	5%	42%	28%	19%	6%	100%
SW Tarlong	296	216	3%	24%	44%	25%	4%	100%
N Tarlong	826	514	2%	21%	23%	26%	28%	100%
NE Tarlong	110	66	11%	35%	30%	6%	18%	100%
Total	3247	1260						
Normalized phytoclasts				28%	31%	23%	17%	

TABLE 3.—*The distribution of permineralized wood and adpression assemblages in the studied sections, parsed by the number of occurrences assigned to depositional environment and the interpretation of climate under which these were preserved. EOD: Braided = braided river; Meandering = meandering river; Lake Delta = shallow, lake-margin deltaic sediments; Lake margin, non-deltaic = lakeplain-littoral with or without a maximum-transgressive shale present in the HC. Climate: A-SA = arid to semi-arid; SA-SH = semi-arid to subhumid; SH-H = subhumid to humid.*

Permineralized/Woody	Braided	Meandering	Lake Delta	Profundal Lake	A-SA	SA-SH	SH-H
Dalongkuo North		4				1	3
Dalongkuo South		4	1				5
Zhaobishan	2	1	1	1			5
South Tadongguo		4	1		2	3	
Central/North Tarlong				5	1	3	1
Southwest Tarlong				1			1
South Tarlong				1			1
NE Tarlong		2	1				3
North Tarlong		1	1	1			3
Proportion	6%	50%	16%	28%	9%	22%	69%
Adpressions	Braided	Meandering	Lake Delta	Profundal Lake	A-SA	SA-SH	SH-H
Dalongkuo North	1			3		3	1
Dalongkuo South		1		4		3	2
Zhaobishan							
South Tadongguo		1					1
Central/North Tarlong				1			1
Southwest Tarlong		1	1				2
South Tarlong			1	1			2
NE Tarlong							
North Tarlong			4	2			5
Proportion	0%	14%	29%	52%	0%	30%	70%

lacustrine deltaic deposits (e.g., Spicer and Wolfe 1987), and bottom sediments in lakes (e.g., Spicer 1991). In contrast, the near ubiquitous nature of heteromeric and isomeric debris fields, preserved as drapes on fluvial and lacustrine bedding (Table 2), provides evidence that does not support an interpretation of vegetational demise followed by long-term recovery across the crisis interval.

The presence of phytoclast (mesofossil) assemblages—commonly not reported, utilized, or accounted for—attest to several facts. First, sufficient biomass grew along waterways to contribute a supply of organic detritus to these continental systems consistently over time. It has been shown that riparian biomass is the primary source for organic contribution to fluvial and limnic systems, and the contribution from non-riparian, interfluvial (floodplain) vegetation is insignificant (e.g., Gastaldo et al. 1987, 1989). Ultimately, a very small percentage of transported biomass settled to the sediment-water interface either in meandering river, littoral and sublittoral lake, or lacustrine deltaic deposits (Table 3). In the case of rivers, variable discharge over the life of any channel or channel system reworked bedload, re-suspending and mechanically fragmenting detritus which, ultimately, settled in hydrodynamic equivalency with micaceous minerals as drapes on bedding. In the case of rift lakes, the redistribution of sediments by turbidity currents (Zhang and Scholz 2015) results in similar accumulations on laminated bedding. Although systematic information can be obtained from these mesofossil assemblages, such investigations, to date, have centered on bedding whereupon either cuticular remains (e.g., Cai et al. 2019) or charcoal occurs (e.g., Cai et al. 2021). Second, similar pore-water geochemistries existed in both depositional environments at various points in time, promoting the decay (carbon films) or preservation (individual fragments) of phytoclast assemblages. Third, the absence of adpression or phytoclast assemblages in river-and-lake deposits is more likely related to physical (e.g., variable discharge water velocities and bedload grain size, bottom-water geochemistry including pore-water oxygenation) or geographical factors (e.g., variation and style of in-channel barforms and distance from shoreline) than it is to an absence of organic-matter contribution.

The nature of fluvial sediments and their clast-size distribution (conglomerate and coarse-to-medium-grained sand versus fine-grained sand and silt) control both the processes that mechanically degrade and fragment plant parts during bedload transport (Gastaldo 1994) and, in large part, control the distribution of palynomorphs (Gastaldo 2012). Although biochemical alteration and cellular lysis can occur to plant debris during suspension-load transport, floating on or within the water column does not promote fragmentation, which may be facilitated by invertebrate or vertebrate activity. The nature of fluvial sediments also influences subsequent oxygenation, redox, and pore-water chemistries following burial (Gastaldo and Huc 1992). It is not surprising that there are no adpression and few phytoclast assemblages (Tables 2, 3) reported in HCs characterized by coarse-grained river deposits (e.g., Jiucaiyuan and Shaofanggou LCs; Table 1). In contrast, fine-grained rift-lake sediments, deposited under semi-humid to humid conditions, have a higher potential to preserve adpression assemblages. Yet, these occur rarely in HC lake-bed sediments (e.g., Wutonggou LC; Table 1). Their absence is likely a function of several factors that operated in tandem over space and time.

Macroscopic debris (leaves, stems/trunks, reproductive structures) transported in suspension in streams/rivers and debouched into any lake may either accumulate in lake-delta deposits, in response a change in velocity as they enter a standing body of water (e.g., Spicer 1981, 1989; Spicer and Wolfe 1987), or will disperse, rather than concentrate, across the surface of the water body. As such, the number of potential fossils per unit hectare of open-water, bottom sediment is dependent on at least two other variables. The first is the extent of the regional drainage system that transports debris into the lake which, even when the organic load might have been unusually high (e.g., traumatic generation of aerial plant parts associated with storms; Gastaldo 1990), may be significantly low when dispersed prior to settling to the sediment-water interface. The second is the density of shoreline vegetation that might contribute aerial detritus

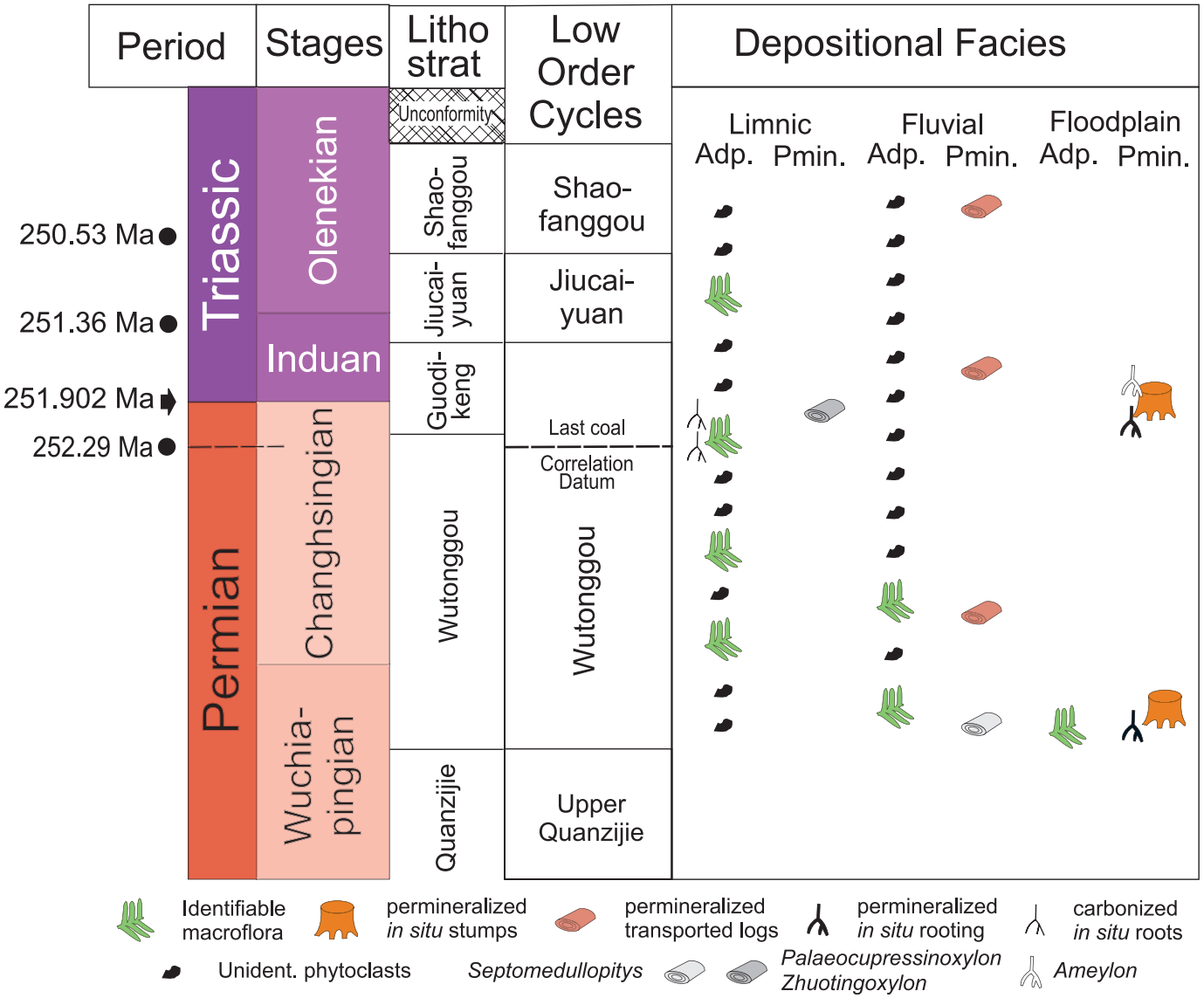

FIG. 13.—Summary diagram showing the distribution of plant taphonomic assemblages in the upper Permian and Lower Triassic depositional regimes of the Bogda Mountains, NE Xinjiang Uyghur Autonomous Region, China. Note that only reports of permineralized *in situ* rooting structures are depicted; carbonized roots and rootlets, root halos, calcified vertical rooting and rhizoconcretions occur throughout the stratigraphic succession (see Thomas et al. 2011; Yang et al. 2021). Abbreviations: Adp = adpression; Pmin = permineralized. Black circle age assignments of LCs follow Yang et al. (2021); black arrow age assignment of the Permian–Triassic Boundary follows ICS chart 2022/v2 (Cohen et al. 2013, updated).

directly to the lake, and actual perimeter of the water body, itself (Spicer 1989). Prevailing water chemistries will control preservation potential once debris arrives at the sediment-water interface, and these are not uniform in any lake. Water chemistry is constrained primarily by distance from shoreline, water temperature, evaporative conditions, and, ultimately, water depth. Oxygenated bottom waters promote aerobic microbial and invertebrate activity which, in turn, utilize and degrade the organic resource in the Taphonomically Active Zone (TAZ; e.g., Martin 1999). This results in extremely low preservation potential unless increased, contemporaneous sediment supply buries the debris below the TAZ, insulating it from degradation and/or promoting the development of a biofilm-enhanced envelope (e.g., Dunn et al. 1997; Locatelli et al. 2017). Dysoxic and anoxic bottom-water conditions at depth generally increase preservation potential, although such depths in rift lakes commonly are several kilometers distant from any shoreline and terrestrial input. For example, modern Lake Tanganyika is 85 km wide and 635 km long during pluvial periods. Here, the oxygen-minimum zone (OMZ) is first encountered at depths of 80–100 m at variable distances from shoreline (Degens et al. 1971). During the 106 ka megadrought when the width of the lake shrunk to 30 km and its length to ~ 500 km, similar OMZ depths are recorded although at different geographic positions in the basin (McGlue et al. 2008). Hence, there is a very low probability that terrestrial megafloral remains could be expected in any specific collection site with an understanding of these constraints acknowledging the size of the water body and the uneven distribution of conditions under which preservation can be promoted. It is not surprising, then, there is a reported absence of terrestrial debris assemblages in modern rift-lake deposits (e.g., Verschuren et al. 2001). Other taphonomic constraints exist when considering permineralized wood assemblages.

Woody Debris Trends

Large woody debris is a common constituent of rivers that traverse forested landscapes that have not undergone anthropogenic modification and alteration (Gastaldo 2004; Gastaldo and Degges 2007). Yet, long-term decay processes operating over a span of decades to a few centuries reduce the preservation potential of both logs and woody debris (Burnham 1993) unless these are delignified and subjected to mineralization (Dietrich et al. 2015). There appears to be an underlying, and unstated, assumption in some literature that the probability of permineralized wood occurrence is equal over space and time. Hence, its absence in a stratigraphic interval is the consequence of a sudden catastrophic event affecting standing biomass (e.g., Cao et al. 2019). Yet, the geochemical conditions under which woody tissues are permineralized are an anomaly, rather than a preservational uniformity (Hellawell et al. 2015; Gee and Leisegang 2021). Woody debris must be entombed in sediment where pore-water chemistries promote mineralization on either lignified (Mustoe 2017) or previously delignified cell walls (Dietrich et al. 2015). And, those pore-water chemistries must be sufficiently mineral-rich, being sustained over years to decades, for wood to scavenge silica complexes and precipitate them on organic surfaces inside xylem cells (Ballhaus et al. 2012). Permineralization advances at a higher rate when wood is adjacent to thermal hot springs (Akahane et al. 2004) or ash beds (Ballhaus et al. 2012). Hence, the conditions under which permineralization of wood can proceed are not met uniformly across space and time, a fact that is reflected in its distribution in the Bogda stratigraphic successions. Not only does a lithofacies association fundamentally control the frequency of occurrence of a continental taphonomic assemblage, but autogenic (e.g., hot springs) and allogenic (e.g., explosive volcanic activity) mechanisms play the fundamental role for when, and if, woody debris might be permineralized (see Spicer 1989; Ballhaus et al. 2012; Hellawell et al. 2015). The sporadic occurrence of this taphonomic assemblage in the Bogda succession evidences the rarity of this preservational mode (Fig. 13) because silicate permineralization requires an alkaline (to take silica into solution) to acidic (to precipitate silica—often acidity rises with partial decay) shift in pore waters, which can be driven by cycles in seasonal temperature, precipitation and/or evaporation cycles (e.g., Leo and Barghoorn 1976).

Floral Trends and Climate

Although our data are limited, there is a strong correlation between megafloral assemblages and the climatic conditions under which these were preserved. Two thirds of permineralized wood and adpression assemblages occur in HCs interpreted to have accumulated under semi-humid to humid conditions (Table 1). A lower proportion of these assemblages are found in HCs interpreted as having experienced semi-arid to semi-humid conditions, and only a few occurrences of permineralized wood are restricted to arid to semi-arid intervals. Hence, when combined with the discussion above, it becomes clear that the taphonomic "window" within which megafloral assemblages can become part of the stratigraphic record also is very limited.

In contrast, the presence of phytoclast drapes on bedding surfaces is controlled both by the available sediment-grain size of the depositional setting and climate. These assemblages are found across the interpreted climate spectrum, but are rarely encountered in HCs that accumulated under either arid to semi-arid conditions (3%) or semi-arid to subhumid conditions (8%; see Online Supplemental File). The range of phytoclast assemblage categories, from concentrated to disseminated, predominate in HCs that accumulated under subhumid to humid conditions (89%), which parallels our observations on adpression assemblages. The predominance of both adpression and phytoclast assemblages developed under these climates is expected, because of increased sediment load associated with seasonal rainfall patterns (DiMichele and Gastaldo 2008, p. 155). Where evaporation exceeds rainfall, under more subhumid to sub-arid conditions, the dearth of phytoclast draped bounding surfaces in fluvial sediments is likely a function of taphonomy—geochemical conditions promoting decay—rather than an absence of vegetation on the landscape. Hence, when climate conditions are more seasonal there is a higher probability of plant preservation and phytoclast assemblages are common. Conversely, when climate conditions are nonseasonal or aseasonal (sub-arid to arid), plant preservation potential is very low and phytoclast assemblages are rare.

General Taphonomic Patterns

Behrensmeyer and Hook (1992) presented a discussion, and series of tables, documenting the most common types of organic remains preserved across the array of terrestrial environments and subenvironments. The reader is directed to comprehensive discussions in Spicer (1989, 1991), Greenwood (1991), Behrensmeyer et al. (2000), and DiMichele and Gastaldo (2008) for additional information. Depositional environments in which fossils are commonly preserved include active-and-abandoned channel and anoxic lake deposits. Today, woody detritus accumulates both in channel-lag deposits and barforms of various configurations, whereas leaves and phytoclasts may be common in fine-grained barform troughs, which is the case for Wuchiapingian-aged plant assemblages encountered in the current study. Deep lake deposits often are void of megafloral elements, for reasons given above. But, these settings can preserve unique assemblages especially under conditions of high productivity above an anoxic hypolimnion, resulting in organic-rich black shales. Although black shales encountered, to date, in the rift-lake sediments of the Bogda Mountains preserve conchostrachans (unpublished), fragmented and moderate-to-poorly preserved plant remains rarely are encountered in Changhsingian (e.g., Fig. 7) and Induan (Fig. 12) lakes. In contrast, there is little evidence for their presence in lithologies that represent sediments subjected to subaerial exposure.

Pedogenesis of overbank (floodplain) deposits, across both modern and deep-time floodplains, promotes soft tissue decay and organic recycling. Recognizable or identifiable soft plant tissues are preserved as carbon films, root halos, or traces (Behrensmeyer and Hook 1992), with a higher probability (Regan et al. 2022), in hydromorphic (Fig. 5) and organic-rich facies (Fig. 8) than in well-drained soils formed. Immature soils are more common in aggradational landscapes, whereas better-drained soils are a consequence of floodplain stasis (DiMichele and Gastaldo 2008). When rooting structures are encountered in paleosols, these may be enhanced by mineral precipitation in either poorly drained Protosols (siderite) or well-drained, calcium-rich Vertisols or Calcisols (calcite; see Online Supplemental File). In contrast, the isolated and rare occurrences of autochthonous burial of erect trees (Figs. 5, 6) rooted in their paleosol is the result of a rapid change in base-level (commonly a consequence of earthquake activity), genesis of accommodation, accompanying high rates of sedimentation (Gastaldo et al. 2004), and a regional reset of the watertable (Gastaldo and Demko 2011).

CONCLUSIONS

The plant taphonomic character of uppermost Permian and Lower Triassic strata, encompassing nearly 5 km of measured section, are assessed in the Bogda Mountains, Xinjiang Province, western China. These sediments were deposited in the middle paleolatitudes of NE Pangea beginning in the latest Carboniferous and terminating in the Middle Triassic. Rocks assigned to the Wutonggou and the lower Guodikeng formations are Wuchiapingian–Changhsingian in age, whereas the upper Guodikeng and overlying Jiucaiyuan, and Shaofanggou formations are Induan and Olenekian, respectively, in age. These rocks have been parsed into three, low order cycles—Wutonggou, Juicaiyuan, and Shaofanggou—

wherein the Permian–Triassic Boundary is age modeled to occur in the upper Wutonggou LC (Yang et al. 2010, 2021). One thousand eight hundred thirty eight (1838) HCs are recognized based on repetitive changes in sedimentary environments, spread across a geographic area of ~ 100 km distance from west to east, across three graben or half-graben structures. Field observations of the nature of four discrete plant-fossil assemblages originate from HCs and include: woody (permineralized, coalified), identifiable adpression (compression/impression), phytoclast (fragmented, concentrated or disseminated, and unidentifiable), and root structures (carbon films, rootlets, root halos, root molds, calcite-filled tubules, and rhizoconcretions).

Plant fossils, preserved either as adpressions or permineralized wood, account for a very small percentage of intervals. Identifiable plant parts are preserved in <2.5% of HCs, whereas permineralized wood occurs in only 2% of the record in the five localities where all three LCs are exposed. When considering the occurrence of identifiable plants encountered only in the Wutonggou LC, which outcrops in all localities under study and includes the PTB, adpression assemblages represent < 1% of all HC records. In contrast, permineralized wood assemblages occur in < 2% of HCs. Adpression assemblages are found in fine-grained sediments of: (1) fluvial deposits, concentrated in channel bases, or trough fills in cross-bed sets; (2) rift-lake laminae likely associated with (e.g., Gilbert-type) deltaic deposits; and, rarely, as (3) degraded litters of paleosols. In contrast, permineralized wood assemblages are most often preserved in coarser-grained sediments including basal channel-lag deposits and barforms in conglomeratic sandstone bodies. These fluvial systems, though, were deposited under semi-humid to humid climates. In only two instances, in two separate localities, are autochthonous tree stumps preserved upright, with their rooting systems entombed in the underlying paleosol.

Rooting structures are preserved in < 25% of HCs and are confined, with few exceptions, to paleosol intervals. Yet, this assemblage is not found equally throughout the stratigraphy and across the region. Rooting structures are preserved more commonly in the Triassic successions of the Juicaiyuan and Shaofanggou LCs where there is a lower frequency of either adpressions or permineralizations. Stating the obvious, these data are either a function of where stratigraphic sections were measured and the incidence that paleosols of various character were intercepted in those transects, the greater development of paleosols during the final histories of graben and half-graben successions, or a combination of both factors.

The most ubiquitous, consistent, and often encountered taphonomic assemblage is that of phytoclasts. This category is preserved as either heteromeric or isomeric assemblages, concentrated, dispersed, or disseminated atop bedding surfaces of bedform structures in fluvial or rift-lake deposits. Forty-three percent of HCs in the study interval are reported to preserve such mesofossil assemblages, generally restricted to fine and very fine (lithic) sandstone, siltstone, shale, and mudstone. Phytoclast assemblages are found in 54% of Wutonggou HCs and are preserved in intervals below, spanning, and overlying the age-modeled PTB. Hence, these phytoclast assemblages constitute the physical evidence for the presence of riparian vegetation in the landscape during this critical interval where no physical evidence of megafloral remains exists. Due to a near absence of megaflora and the predominance of phytoclast assemblages, deciphering vegetational trends in this region, and elsewhere, must rely on palynological and mesofossil trends to decode and explain extirpations and extinctions of terrestrial plants prior, during, and after the Permian–Triassic crisis.

ACKNOWLEDGMENTS

The authors want to thank the following individuals who provided assistance with the 2019 field excursion: Profs. S. Shen and J. Wang, and L. Liu, Nanjing; S.W. Wu, Z.UY, Ju, W. Zhang, and Y. Lu, Missouri University of Science and Technology; and S.W. Mei and J.J. Li, Nanjing, for logistic support. We appreciate the thoughtful reviews by Robert A. Spicer, an anonymous reviewer, and the journal editors who helped us clarify manuscript text. The project was supported, in part, by: U.S. NSF grants (EAR 1714749 to WY, EAR 171475 to RAG); and the National Natural Science Foundation of China (41872013) and Youth Innovation Promotion Association CAS (2020312) to MW. Acknowledgment is made to the Donors of the American Chemical Society Petroleum Research Fund for partial support of this research to WY.

SUPPLEMENTAL MATERIAL

Data are available from the PALAIOS Data Archive: https://www.sepm.org/supplemental-materials

REFERENCES

Afonin, S.A. and Foster, C.B., 2005, Palynological assemblages and Permian–Triassic boundary in continental deposits of Dalongkou section (Xinjiang, N.-W., China), *in* S.A. Afonin and P.N. Tokarev (eds.), XI All-Russian Palynological Conference "Palynology: Theory and Applications, Proceedings of the Conference 27th September–1st October, Moscow": Russian Academy of Science, Palaeontological Institute, Moscow, p. 14–18. (In Russian).

Akahane, H., Furuno, T., Miyajima, H., Yoshikawa, T., and Yamamoto, S., 2004, Rapid wood silicification in hot spring water: an explanation of silicification of wood during the Earth's history: Sedimentary Geology, v. 169, p. 219–228, doi: 10.1016/j.sedgeo.2004.06.003.

Ballhaus, C., Gee, C.T., Bockrath, C., Greef, K., Mansfeldt, T., and Rhede, D., 2012, The silicification of trees in volcanic ash: an experimental study: Geochimica et Cosmoschimica Acta, v. 84, p. 62–74, doi: 10.2110/palo.2012.p12-064r.

Behrensmeyer, A.K. and Hook, R.W., Rapporteurs, 1992, Paleoenvironmental Contexts and Taphonomic Modes in the Terrestrial Fossil Record, *in* A. Behrenmeyer, J. Damuth, W.A. DiMichele, R. Potts, H.-D. Sues, and S. Wing (eds.), Terrestrial Ecosystems Through Time: University of Chicago Press, Chicago, p. 15–138.

Behrensmeyer, A.K., Kidwell, S.M., and Gastaldo, R.A., 2000, Taphonomy and paleobiology: Paleobiology, v. 26, p. 103–147.

Benton, M. and Newell, A., 2014, Impacts of global warming on Permo–Triassic terrestrial ecosystems: Gondwana Research, v. 25, p. 1308–1337, doi: 10.1016/j.gr.2012.12.010.

Bohacs, K.M., Carroll, A.R., Neal, J.E., and Mankeiwicz, P.J., 2000, Lake basin type, source potential, and hydrocarbon character: an integrated sequence-stratigraphic-geochemical framework, *in* E.H. Gierlowski-Kordesch and K.R. Kelts (eds.), Lake Basins Through Space and Time: AAPG Studies in Geology, v. 46, p. 3–34.

Bourquin, S., Rossignol, C., Jolivet, M., Poujol, M., Broutin, J., and Yu, J., 2018, Terrestrial Permian–Triassic boundary in southern China: new stratigraphic, structural and palaeoenvironment considerations: Palaeogeography, Palaeoclimatology, Palaeoecology, v. 490, p. 40–652, doi: 10.1016/j.palaeo.2017.11.055.

Burnham, R.J., 1990, Paleobotanical implications of drifted seeds and fruits from modern mangrove litter, Twin Cays, Belize: PALAIOS, v. 5, p. 364–370.

Burnham, R.J., 1993, Time resolution in terrestrial macrofloras: guidelines from modern accumulations: Short Courses in Paleontology, Paleontological Society, v. 6, p. 57–78.

Burgess, S.D., Bowring, S., and Shen, S.-Z., 2014, High-precision timeline for Earth's most severe extinction: Proceedings of the National Academy of Sciences of the United States of America, v. 111, p. 3316–3321, doi: 10.1073/pnas.1317692111.

Cai, Y-F., Zhang, H., Feng, Z., Cao, C-Q., and Zheng, Q-F., 2019, A *Germaropteris*-dominated flora from the upper Permian of the Dalongkou section, Xinjiang, Northwest China, and its paleoclimatic and paleoenvironmental implications: Review of Palaeobotany and Palynology, v. 266, p. 61–71, doi: 10.1016/j.revpalbo.2019.01.006.

Cai, Y.-F., Zhang, H., Cao, C.-Q., Zheng, Q.-F., Jin, C.-F., and Shen, S.-Z., 2021, Wildfires and deforestation during the Permian–Triassic transition in the southern Junggar Basin, Northwest China: Earth-Science Reviews, v. 218, article 103670, doi: 10.1016/j.earscirev.2021.103670.

Cao, Y., Song, H., Algeo, T.J., Chu, D., Du, Y., Tian, L, Wang, Y., and Tong, J. 2019, Intensified chemical weathering during the Permian–Triassic transition recorded in terrestrial and marine successions: Palaeogeography, Palaeoclimatology, Palaeoecology, v. 519, p. 166–177, doi: 10.1016/j.palaeo.2018.06.012.

Chu, D., Yu, J., Tong, J., Benton, M., Song, H., Huang, Y., Song, T., and Tian, L., 2016, Biostratigraphic correlation and mass extinction during the Permian–Triassic transition in terrestrial-marine siliciclastic settings of South China: Global and Planetary Change, v. 146, p. 67–88. doi: 10.1016/j.gloplacha.2016.09.009.

Cohen, K.M., Finney, S.C., Gibbard, P.L., and Fan, J.-X., 2013 (updated), The ICS International Chronostratigraphic Chart: Episodes, v. 36, p. 199–204.

Davydov, V.I., Karasev, E.V., Nurgalieva, N.G., Schmitz, M.D., Budnikov, I.V., Biakov, A.S., Kuzina, D.M., Silantiev, V.V., Urazaeva, M.N., Zharinova, V.V., Zorina, S.O., Gareev, B., and Vasilenko, D.V., 2021, Climate and biotic evolution during the Permian–Triassic transition in the temperate Northern Hemisphere, Kuznetsk Basin, Siberia,

Russia: Palaeogeography, Palaeoclimatology, Palaeoecology, v. 573, article 110432, doi: 10.1016/j.palaeo.2021.110432.

Degens, E.T., Von Herzen, R.P., and Wong, H.K., 1971, Lake Tanganyika: water chemistry, sediments, geological structure: Naturwissenschaften, v. 58, p. 229–241, doi: 10.1007/BF00602986

Dietrich, D., Viney, M., and Lempke, T., 2015, Petrifactions and wood-templated ceramics: comparisons between natural and artificial silicification: International Association of Wood Anatomists, v. 36, p. 167–185, doi: 10.1163/22941932-00000094

DiMichele, W.A. and Gastaldo, R.A., 2008, Plant paleoecology in deep time: Annals of the Missouri Botanical Gardens, v. 95, p. 144–198.

DiMichele, W.A., Bashforth, A.R., Falcon-Lang, H.J., and Lucas, S.G., 2020, Uplands, lowlands, and climate: taphonomic megabiases and the apparent rise of a xeromorphic, drought-tolerant flora during the Pennsylvanian–Permian transition: Palaeogeography, Palaeoclimatology, Palaeoecology, v. 559, article 109965, doi: 10.1016/j.palaeo.2020.109965.

Dunn, K., McLean, R., Upchurch, G., and Folk, R., 1997, Enhancement of leaf fossilization potential by bacterial biofilms: Geology, v. 25, p. 1119–1122, doi: 10.1130/0091-7613(1997)025.

Fielding, C.R., Frank, T.D., Savatic, K., Mays, C., McLoughlin, S., Vajda, V., and Nicoll, R.S., 2022, Environmental change in the late Permian of Queensland, NE Australia: the warmup to the end-Permian Extinction: Palaeogeography, Palaeoclimatology, Palaeoecology, v. 594, article 110936, doi: 10.1016/j.palaeo.2022.110936.

Foster, C.B. and Afonin, S.A., 2006, *Syndesmorion* gen. nov.—a coenobial alga of Chlorococcalean affinity from the continental Permian–Triassic deposits of Dalongkou section, Xinjiang Province, China: Review of Palaeobotany and Palynology, v. 138, p. 1–8.

Gastaldo, R.A., 1988, A conspectus of phytotaphonomy, *in* W.A. DiMichele and S.L. Wing (eds.), Methods and Applications of Plant Paleoecology: Notes for a Short Course, Paleontological Society Special Publication 3, p. 14–28

Gastaldo, R.A., 1989, Preliminary observations on phytotaphonomic assemblages in a subtropical/temperate Holocene bayhead delta: Mobile Delta, Gulf Coastal Plain, Alabama: Review of Palaeobotany and Palynology, v. 58, p. 61–84.

Gastaldo, R.A., 1990, The paleobotanical character of log assemblages necessary to differentiate blow-downs resulting from cyclonic winds: PALAIOS, v. 5, p. 472–478.

Gastaldo, R.A., 1994, The genesis and sedimentation of phytoclasts with examples from coastal environments, *in* A. Traverse (ed.) Sedimentation of Organic Particles: Cambridge University Press, New York, Chapter 7, p. 103–127.

Gastaldo, R.A., 2004, The relationship between bedform and log orientation in a Paleogene fluvial channel, Weißelster basin, Germany: implications for the use of coarse woody debris for paleocurrent analysis: PALAIOS, v. 19, p. 595–606.

Gastaldo, R.A., 2012, Taphonomic controls on the distribution of palynomorphs in tidally-influenced coastal deltaic settings: PALAIOS, v. 27, p. 798–810. doi:10.2110/palo.2012.p12-030r

Gastaldo, R.A. and Huc, A.Y., 1992, Sediment facies, depositional environments, and distribution of phytoclasts in the Recent Mahakam River delta, Kalimantan, Indonesia: PALAIOS, v. 7, p. 574–591.

Gastaldo, R.A., Stevanovic-Walls, I., and Ware, W.N., 2004, *In situ*, erect forests are evidence for large-magnitude, coseismic base-level changes within Pennsylvanian cyclothems of the Black Warrior Basin, USA, *in* J.C. Pashin and R.A. Gastaldo (eds.), Coal-Bearing Strata: Sequence Stratigraphy, Paleoclimate, and Tectonics: AAPG Studies in Geology, v. 51, p. 219–238.

Gastaldo, R.A. and Degges, C.W., 2007, Sedimentology and paleontology of a Carboniferous log jam: International Journal of Coal Geology, v. 69, p. 103–118.

Gastaldo, R.A. and Demko, T.M., 2011, Long term hydrology controls the plant fossil record, *in* P.A. Allison and D.J. Bottjer (eds.), Taphonomy (second edition): Processes and Bias Through Time: Topics in Geobiology, v. 32, p. 249–286, doi: 10.1007/978-90-481-8643-3_7).

Gastaldo, R.A., Douglass, D.P., and McCarroll, S.M., 1987, Origin, characteristics and provenance of plant macrodetritus in a Holocene crevasse splay, Mobile delta, Alabama: PALAIOS, v. 2, p. 229–240.

Gastaldo, R.A., Bearce, S.C., Degges, C., Hunt, R.J., Peebles, M.W., and Violette, D.L., 1989, Biostratinomy of a Holocene oxbow lake: a backswamp to mid-channel transect: Review of Palaeobotany and Palynology, v. 58, p. 47–60.

Gastaldo, R.A., Adendorff, R., Bamford, M.K., Labandeira, Neveling, J., and Sims, H.J., 2005, Taphonomic trends of macrofloral assemblages across the Permian–Triassic Boundary, Karoo Basin, South Africa: PALAIOS, v. 20, p. 478–497, doi: 10.1016/j.palaeo.2010.03.052.

Gastaldo, R.A., Purkyňová, E., Šimůnek, Z., and Schmitz, M.D., 2009, Ecological persistence in the Late Mississippian (Serpukhovian–Namurian A) megafloral record of the Upper Silesian Basin, Czech Republic: PALAIOS, v. 24, p. 336–350.

Gastaldo, R.A., Tabor, N., and Neveling, J., 2020, Trends in Late Permian (Changhsingian) paleoclimate in the *Daptocephalus* Assemblage Zone, Eastern Cape Province, South Africa: Frontiers in Earth Science, v. 8, article 567109.

Gastaldo, R.A., Neveling, J., Geissman, J.W., Kamo, S.L., and Looy, C.V., 2021, A tale of two Tweefonteins: what physical correlation, geochronology, magnetic polarity stratigraphy, and palynology say about the end-Permian terrestrial extinction paradigm: Geological Society of America Bulletin, v. 133, https://doi.org/10.1130/B35830.1/5345349/b35830.pdf

Gee, C T. and Liesegang, M., 2021, Experimental silicification of wood in the lab and field: Pivotal studies and open questions, *in* C.T. Gee, V.E. McCoy, and P.M. Sander (eds.), Fossilization: Understanding the Material Nature of Ancient Plants and Animals: John Hopkins University Press, Baltimore, MD, p. 139–158.

Greb, S.F., DiMichele, W.D., and Gastaldo, R.A., 2006, Evolution of wetland types and the importance of wetlands in Earth history, *in* W.A. DiMichele and S. Greb (eds.), Wetlands Through Time: Geological Society of America, Special Publication, v. 399, p. 1–40.

Greb, S.F., DiMichele, W.A., Gastaldo, R.A., Eble, C.F., and Wing, S.L., 2022, Prehistoric Wetlands, *in* T. Mehner and K. Kockner (eds.), Encyclopedia of Inland Waters (second edition): Elsevier (print on demand), v. 3, p. 23–32, doi: 10.1016/B978-0-12-819166-8.00066-9.

Greenwood, D.R., 1991, The taphonomy of plant macrofossils, *in* S.K. Donovan (ed.), The Processes of Fossilization: Belhaven Press, London, p. 141–169.

Hellawell, J., Ballhaus, C., Gee, C.T., Mustoe, G.E., Nagel, T.J., Wirth, R., Rethemeyer, J., Tomaschek, F., Geisler, T., Greef, K., and Mansfeldt, T., 2015, Silicification of recent conifer wood at a Yellowstone hot spring: Geochimica et Cosmochimica Acta, v. 149, p. 79–87.

Leo, R.F. and Barghoorn, E.S., 1976, Silicification of wood: Botanical Museum Leaflets, Harvard University, v. 25, p. 1–46.

Locatelli, E., McMahon, S., and Bilger, H., 2017, Biofilms mediate the preservation of leaf adpression fossils by clays: PALAIOS, v. 32, p. 708–724, doi: 10.2110/palo.2017.043.

Lucas, S., 2021, Nonmarine mass extinctions: Paleontological Research, v. 25, p. 329–344, doi: 10.2517/2021PR004.

Martin, R.E., 1999, Taphonomy: A Process Approach: Cambridge Paleobiology Series, Cambridge, n. 4, 526 p., doi: 10.1017/CBO9780511612381.

McGlue, M.M., Lezzar, K.E., Cohen, A.S., Russell, J.M., Tiercelin, J.J., Felton, A.A., Mbede, E., and Nkotagu, H.H., 2008, Seismic records of late Pleistocene aridity in Lake Tanganyika, tropical East Africa: Journal of Paleolimnology, v. 40, p. 635–653.

Metcalfe, I., Foster, C.B., Afonin, S.A., Nicoll, R.S., Mundil, R., Wang Xiaofeng, and Lucas, S.G., 2009, Stratigraphy, biostratigraphy and C-isotopes of the Permian–Triassic non-marine sequence at Dalongkou and Lucaogou, Xinjiang Province, China: Journal of Asian Earth Sciences, v. 36, p. 503–520.

Miller, A.I. and Foote, M., 1996, Calibrating the Ordovician radiation of marine life: implications for Phanerozoic diversity trends: Paleobiology, v. 22, p. 304–309.

Montañez, I., McElwain, J., Poulsen, C., White, J.D., DiMichele, W.A., Wilson, J.P., Griggs, G., and Hren, M.T., 2016, Climate, pCO^2 and terrestrial carbon cycle linkages during late Palaeozoic glacial-interglacial cycles: Nature Geoscience, v. 9, p. 824–828, doi: 10.1038/ngeo2822.

Mustoe, G.E., 2017, Wood petrifaction: a new view of permineralization and replacement: Geosciences, v. 7, p. 119, doi: 10.3390/geosciences7040119.

Nowak, H., Schneebeli-Hermann, E., and Kustatscher, E., 2019, No mass extinction for land plants at the Permian–Triassic transition: Nature Communications, v. 10, p. 384.

Obrist-Farner, J. and Yang, W., 2015, Implications of loess and fluvial deposits on paleoclimatic conditions during an icehouse-hothouse transition, Capitanian upper Quanzijie low-order cycle, Bogda Mountains, NW China: Palaeogeography, Palaeoclimatology, Palaeoecology, v. 441, p. 959–981, doi: 10.1016/j.palaeo.2015.10.041.

Obrist-Farner, J. and Yang, W., 2017, Provenance and depositional conditions of fluvial conglomerates and sandstones and their controlling processes in a rift setting, mid-Permian lower and upper Quanzijie low order cycles, Bogda Mountains, NW China: Journal of Asian Earth Sciences, v. 138, p. 317–340.

Raup, D.M., 1972, Taxonomic diversity during the Phanerozoic: Science, v. 177, p. 1065–1071.

Regan, A.K., Rogers, R.R., and Holland, S.M., 2022, Quantifying controls on the occurrence of nonmarine fossils: Geology, v. 50, p. 1287–1290, doi: 10.1130/G50254.1.

Ricardi-Branco, F., Rios, F.S., and Pereira, S.Y., 2020, Actualistic taphonomy of plant remains in tropical forests of southeastern Brazil, *in* S. Martínez, A. Rojas, and F. Cabrera (eds.), Actualistic Taphonomy in South America: Topics in Geobiology, v. 48, p. 111–138, doi: 10.1007/978-3-030-20625-3_7.

Roopnarine, P.D., Angielczyk, K.D., Weik A., and Dineen, A., 2019, Ecological persistence, incumbency and reorganization in the Karoo Basin during the Permian–Triassic transition: Earth-Science Reviews, v. 189, p. 244–263, doi: 10.1016/j.earscirev.2018.10.014.

Rygel, M.C., Gibling, M.R., and Calder, J.H., 2004, Vegetation-induced sedimentary structures from fossil forests in the Pennsylvanian Joggins Formation, Nova Scotia: Sedimentology, v. 51, p. 531–552, doi: 10.1111/j.1365-3091.2004.00635.x.

Schneebeli-Hermann, E., 2020, Regime shifts in an Early Triassic subtropical ecosystem: Frontiers in Earth Science, v. 8, doi: 10.3389/feart.2020.588696.

Scheihing, M.H. and Pfefferkorn, H.W., 1984, The taphonomy of land plants in the Orinoco delta: a model for the incorporation of plant parts in clastic sediments of Late Carboniferous age of Euramerica: Review of Palaeobotany and Palynology, v. 41, p. 205–240, doi: 10.1016/0034-6667(84)90047-2.

Şengör, A.M.C. and Natalín, B.A., 1996, Palaeotectonics of Asia: fragments of a synthesis, *in* A. Yin and M. Harrison (eds.), The Tectonic Evolution of Asia, Rubey Colloquium, Cambridge University Press, Cambridge, p. 486–640.

Shao, L., Stattegger, K., and Garbe-Schoenberg, C.-D., 2001, Sandstone petrology and geochemistry of the Turpan Basin (NW China): implications for the Tectonic evolution of a continental basin: Journal of Sedimentary Research, v. 71, p. 37–49.

Shen, S.Z., Ramezani, J., Chen, J., Cao, C.Q., Erwin, D.H., Zhang, H., Xiang, L., Schoepfer, S.D., Henderson, C.M., Zheng, Q.F., Bowring, S.A., Wang, Y., Li, X.H., Wang, X.D., Yuan, D.X., Zhang, Y.C., Mu, L., Wang, J., and Wu, Y.S., 2019, A sudden end-Permian mass extinction in South China: Geological Society of America Bulletin, v. 131, p. 205–223, doi: 10 .1130 /B31909.1.

Smith, R.M.H. and Botha-Brink, J., 2014, Anatomy of a mass extinction: sedimentological and taphonomic evidence for drought-induced die-offs at the Permian–Triassic boundary in the main Karoo Basin, South Africa: Palaeogeography, Palaeoclimatology, Palaeoecology, v. 316, p. 99–118.

Spicer, R.A., 1981, The sorting and deposition of allochthonous plant material in a modern environment at Silwood Lake, Silwood Park, Berkshire, England: U.S. Geological Survey Professional Paper 1143, 77 p.

Spicer, R.A., 1989, The formation and interpretation of plant fossil assemblages: Advances in Botanical Research, v. 16, p. 95–191.

Spicer, R.A., 1991, Plant Taphonomic Processes, *in* P.A. Allison and D.E.G. Briggs (eds.), Taphonomy: Releasing the Data Locked in the Fossil Record: Plenum Press ,New York, p. 71–113, doi: 10.1007/978-1-4899-5034-5_3.

Spicer, R. and Wolfe, J., 1987, Plant taphonomy of late Holocene deposits in Trinity (Clair Engle) Lake, northern California: Paleobiology, v. 13, p. 227–245, doi: 10.1017/S00 94837300008770.

Staub, J.R. and Gastaldo, R.A., 2003, Late Quaternary incised-valley fill and deltaic sediments in the Rajang River Delta, *in* H.F. Sidi, D. Nummedal, P. Imbert, H. Darman, and H.W. Posamentier (eds.), Tropical Deltas of Southeast Asia—Sedimentology, Stratigraphy, and Petroleum Geology: SEPM Special Publications, v. 76, p. 71–87.

Tabor, N.J., Geissman, J.W., Renne, P.R, Mundil, R., Mitchell, W.S, III, Myers, T.S., Jackson, J., Looy, C.V., and Kirchholtes, R.P., 2022, How to recognize an extinction when there is nothing around to go extinct: evidence of a continuous continental Permian–Triassic Boundary section in the Palo Duro Basin, Northwest Texas, U.S.A.: Frontiers in Science, v. 9, doi: 10.3389/feart.2021.747777.

Thomas, S.G., Tabor, N.J., Yang, W., Myers, T.S., Yang, Y., and Wang, D., 2011, Paleosol stratigraphy across the Permo–Triassic boundary, Bogda Mountains, NW China: implications for palaeoenvironmental transition through earth's largest mass extinction: Palaeogeography, Palaeoclimatology, Palaeoecology, v. 308, p. 41–64, doi: 10.1016/j.palaeo.20.

Verschuren, D., 2001, Reconstructing fluctuations of a shallow East African lake during the past 1800 yrs from sediment stratigraphy in a submerged crater basin: Journal of Paleolimnology, v. 25. p. 297–311.

Viglietti, P.A., Benson, R.B.J., Smith, R.H.H., Botha, J., Kammere, C.F., Skosan, Z., Butler, E., Crean., A., Eloff, B., Kaal, S., Mohoi, J., Molehe, W., Mtalana, N. Mtungata, S., Ntheri, N., Ntsala, T., Nyaphuli, J., October, P., Skinner, G. Strong, M., Stummer, H., Wolvaardt, F.P., and Angielczyk, K.D., 2021, Evidence from South Africa for a protracted end-Permian extinction on land: Proceedings of the National Academy of Sciences of the United States of America, v. 118, e2017045118, doi: 10.1073/pnas.201 7045118.

Wall, P.D., Ivany, L.C., and Wilkinson, B.H., 2009, Revisiting Raup: exploring the influence of outcrop area on diversity in light of modern sample-standardization techniques: Paleobiology, v. 35, p. 146–167.

Wall, P.D., Ivany, L.C., and Wilkinson, B.H., 2011, Impact of outcrop area on estimates of Phanerozoic terrestrial biodiversity trends, *in* A.J. McGowan and A.B. Smith (eds.), Comparing the Geological and Fossil Records: Implications for Biodiversity Studies: Geological Society of London, Special Publications, v. 358, p. 53–62.

Wan, M.L., Yang, W., and Wang, J., 2014, *Septomedullopitys szei* sp. nov., a new Gymnospermous wood from lower Wuchiapingian (upper Permian) continental deposits of NW China, and its implication for a weakly seasonal humid climate in mid-latitude NE Pangaea: Palaeogeography, Palaeoclimatology Palaeoecology, v. 407, p. 1–13, doi: 10.1016/j.palaeo.2014.04.011.

Wan, M.-Li., Zhou, W.-M., Yang, W., and Wang, J., 2016, Charred wood of *Prototaxoxylon* from the Wuchiapingian Wutonggou Formation (Permian) of Dalongkou, northern Bogda Mountains, northwestern China: Palaeoworld, v. 25, p. 21–31, doi: 10.1016/j.palwor.2015.06.003.

Wan, M.L., Yang, W., Liu, L.J., and Wang, J., 2017, *Ductoagathoxylon jimsarensis* sp. nov., a coniferous wood from the Wuchiapingian (upper Permian) Wutonggou Formation in Junggar Basin, northern Bogda Mountains, northwestern China: Review of Palaeobotany and Palynology, v. 241, p. 13–25, doi: 10.1016/j.revpalbo.2017.02.004.

Wan, M., Gastaldo, R.A., and Yang, W., 2019a, Taphonomic and paleoecological aspects of a silicified stand of the gymnosperm *Protophyllocladoxylon* from the Wutonggou Lower Order Cycle, Bogda Mountains, Xinjiang Province, Western China: Geological Society of America Abstracts with Programs, v. 51, no. 5, doi: 10.1130/abs/2019AM-335626.

Wan, M.-Li., Yang, W., and Wang, J., 2019b, *Amyelon bogdense* sp. nov., a silicified gymnospermous root from the Changhsingian-Induan (?) in southern Bogda Mountains, northwestern China: Review of Palaeobotany and Palynology, v. 263, p. 12–27.

Wan, M.-L., Wan Yang, W., and Wang, J., 2020, *Palaeocupressinoxylon uniseriale* n. gen. n. sp., a gymnospermous wood from the upper Permian of Central Taodonggou, southern Bogda Mountains, northwestern China: Palaeoworld, v. 29, p. 117–125.

Wan, M.L., Yang, W., Wang, K.Y., Liu, L.J., and Wang, J., 2021a, *Zhuotingoxylon liaoi* gen. et sp. nov., a silicified coniferous trunk from the Changhsingian (Permian) of southern Bogda Mountains, northwestern China: Geological Journal, v. 56, p. 6135–6150. doi: 10.1002/gj.4189.

Wan, M.L., Yang, W., Wan, S., and Wang, J., 2021b, Wildfires in the Early Triassic of northeastern Pangaea: evidence from fossil charcoal in the Bogda Mountains, northwestern China: Palaeoworld, v. 30, p. 593–601, doi: 10.1016/j.palwor.2021.07.002.

Wing, S.L. and Dimichele, W.A., 1995, Conflict between local and global changes in plant diversity through geological time: PALAIOS, v. 10, p. 551–564, doi: 10.2307/3515094.

Yang, W., 2008, Internal Report—Depositional Systems Analysis within a Seismic Sequence Stratigraphic Framework, Turpan-Hami Basin, NW China: Tu-Ha Oil Company, PetroChina, 129 p., 21 figs., 38 pls.

Yang, W., Feng, Q., Liu, Y.Q., Tabor, N., Thomas, S., Yang, Y., Sun, G.Z., and Sun, B., 2007, Promises and problems of two-dimensional nonmarine sequence stratigraphic analysis using hierarchical depositional cycles—an example from outcrop Lower Permian to Lower Triassic fluvial—lacustrine deposits, Southern Bogda Mountains, Turpan Intermontane Basin, NW China: American Association of Petroleum Geologists Annual Meeting, Long Beach, CA., Abstracts, p. 154.

Yang, W., Feng, Q., Liu, Y.Q., Tabor, N., Miggins, D., Crowley, J.L., Lin, J., and Thomas, S., 2010, Depositional environments and cyclo- and chronostratigraphy of uppermost Carboniferous–lower Triassic fluvial-lacustrine deposits, southern Bogda Mountains, NW China—a terrestrial palaeoclimatic record of mid-latitude NE Pangea: Global and Planetary Change, v. 73, p. 15–113.

Yang, W., Crowley, J.L., Obrist, J., Tabor, N.J., Feng, Q., and Liu, Y.Q., 2013, A marine back-arc origin for the Upper Carboniferous basement of intracontinental greater Turpan- Junggar basin—volcanic, sedimentary, and geochronologic evidence from southern Bogda Mountains, NW China: Geological Society of America Abstracts with Programs, Denver, CO, v. 45, p. 294.

Yang, W., Wan, M., Crowley, J.L., Wang, J., Luo X. Tabor, N.J. Angeilczyk, K.D., Gastaldo, R.A., Geissman, J.W., Liu, F., Roopnarine, P., and Sidor, C., 2021, Paleoenvironmental and paleoclimatic evolution and cyclo- and chrono-stratigraphy of Upper Permian-Lower Triassic fluvial-lacustrine deposits in Bogda Mountains, NW China—implications for diachronous plant evolution across the Permian–Triassic Boundary: Earth Science Reviews, v. 222, article 103741.

Zhang, X. and Scholz, C.A., 2015, Turbidite systems of lacustrine rift basins: examples from the Lake Kivu and Lake Albert rifts, East Africa: Sedimentary Geology, v. 325, p. 177–191, doi: 10.1016/j.sedgeo.2015.06.003.

Zheng, D.Y. and Yang, W., 2020, Provenance of upper Permian–lowermost Triassic sandstones, Wutonggou low-order cycle, Bogda Mountains, NW China: implications on the unroofing history of the Eastern North Tianshan Suture: Journal of Palaeogeography, v. 9, 19 p., doi: 10.1186/s42501-020-00067-9.

Received 1 May 2022; accepted 4 November 2022.